Geophys. J. Int. (2002) **149,** 659–678

Palaeoseismicity studies on end-Pleistocene and Holocene lake deposits around Basle, Switzerland

Arnfried Becker,[1] Colin A. Davenport[2] and Domenico Giardini[1]

[1] *Institut für Geophysik, ETH-Hönggerberg,* CH-8093 *Zürich, Switzerland. E-mail: becker@seismo.ifg.ethz.ch*
[2] *School of Environmental Sciences, University of East Anglia, Norwich* NR4 7TJ, *UK*

Accepted 2001 December 13. Received 2001 September 26; in original form 2001 February 14

SUMMARY

Palaeoseismological investigations in the lakes of Seewen and Bergsee in the Basle region, Switzerland and southern Germany, revealed characteristic event horizons in an otherwise uniform background sedimentary record. Dated and correlated based on radiocarbon ages, palynostratigraphy and sedimentation rates, some of these event horizons show soft-sediment deformation features and fractures that can be interpretated as being the result of earthquake shaking. Two of the event horizons with clear indications for earthquake deformation were detected in both lakes, showing approximately the same age as indicated by radiocarbon dating. A third event horizon with fractures of apparent seismogenic origin, was detected at several drill sites in only one lake (Bergsee). Three further event horizons, two in the Bergsee and one in Lake Seewen, are of uncertain origin, though they show some characteristics that could well be caused by earthquakes. Based on the observations in both lakes, five events were detected of which three are most probably related to earthquakes which occurred between 180 BC–1160 BC, 8260 BC–9040 BC and 10 720 BC–11 200 BC, respectively. The Basle region is well known for the strongest historical earthquake north of the Alps, the AD 1356 Basle earthquake. Based on combined historical and palaeoseismological data, it has been inferred that earthquakes with size comparable to the AD 1356 Basle earthquake have occurred several times within the last 12 000 yr and that the recurrence time for such strong earthquakes are in the range of 1500–3000 yr.

Key words: earthquakes, lake sediments, palaeoseismology, recurrence time, seismic hazard.

1 INTRODUCTION

Palaeoseismic investigations have been successful in many areas of the world in complementing the historical and pre-historical earthquake record allowing a better assessment of the seismic potential of individual seismogenic structures and of the regional seismic hazard (Sims 1975; Doig 1986; Vittori *et al.* 1991; Davenport 1993; Pantosti & Yeats 1993; Boschi *et al.* 1996; Marco *et al.* 1996; Obermeier 1996; Obermeier & Pond 1999). These investigations focus on surface fault reactivation (primary palaeoseismic evidence) (Camelbeeck & Meghraoui 1998) and on a variety of non-primary palaeoseismic evidence (Keefer 1984; Postpischl *et al.* 1991), such as soft-sediment deformation (Rodriguez-Pascua *et al.* 2000).

Because Europe north of the Alps shows a low level of seismicity and crustal deformation, expectations of any results from palaeoseismical investigations have, until recently, been low. Investigations in Sweden in the 1970s and 1980s (Lagerbäck 1978; Mörner 1985; Mörner *et al.* 1989) and Scotland (Ringrose 1989; Davenport *et al.* 1989) have shown that surface fault reactivation and related soft-sediment deformation can be identified under favourable circumstances. However, related earthquake events may have been triggered by late- and post-glacial stress changes in the crust still recovering from the effects of ice-loading. In Central Europe, far from the high-latitude rebound effects, the potential for success increases, particularly where seismogenic sources can be identified, such as in the Rhine Graben system (Lap 1987; Camelbeeck & Meghraoui 1998; Lemeille *et al.* 1999a). The more active terrains adjacent to the Alps have also yielded promising results (Siegenthaler *et al.* 1987; Beck *et al.* 1996; Chapron *et al.* 1999).

The potential for identifying a complete record of major pre-historic events is restricted to areas where the geological record is complete and earthquake-induced deformation structures (seismites) are preserved in a wide range of environments. The northern area of Switzerland, i.e. the city of Basle and its environs, is considered to meet these requirements. Although the instrumental record indicates generally low levels of seismicity, the historical record includes the largest and most damaging earthquake ever recorded in Central–Northern Europe, the AD 1356 Basle event, with an epicentral MSK intensity of IX–X and an estimated magnitude $M_L = 6.5$ (Mayer-Rosa & Cadiot 1979). Today Basle is an

important regional centre with a high population density, key communication nodes, lifelines and critical facilities, with a high concentration of chemical and pharmaceutical industry and four nuclear power stations located within a 50 km distance. It is therefore vital to evaluate accurate exposure scenarios for the Basle region, and in particular, to constrain a possible recurrence time of an AD 1356-type earthquake. As the historical earthquake catalogue covers only the past 1000 yr, additional evidence must be found to establish whether an AD 1356-type event is to be expected once every 1000 or tens of thousands of years.

A variety of palaeoseismological studies are currently focusing on the Basle area. The first investigations carried out in the Dieboldslöchli cave in the Jura Mountains south of Basle (Lemeille *et al.* 1999b) showed regrowth of stalagmites on a fault-plane, suggesting an earthquake event between 1050 and 1400 AD. Additional evidence was found in the Bättlerloch cave, where a laterally displaced fallen block of limestone is overgrown by stalagmites, suggesting an event between 160 BC and 80 AD (Lemeille *et al.* 1999b). Surface faulting was expected as a result of an AD 1356-type earthquake (Meyer *et al.* 1994) and trenching investigations led to the identification of an active surface fault structure south of Basle (Meghraoui *et al.* 2001).

Liquefaction and mass movement in susceptible sedimentary deposits, particularly in lakes, are also expected locally as a consequence of a high level of ground shaking. Mainly because many lakes in Switzerland provide a complete sedimentary record for the Holocene and the latest Pleistocene, we decided to focus our palaeoseismological investigation on lake deposits. Additionally, organic-rich Holocene lake deposits permit high-quality radiocarbon dating, which, when combined with palynostratigraphic evidence, allows the reconstruction of sedimentation rates and the age calibration of lithological profiles. Lake sediments have been investigated to identify and date 'event horizons'. Event horizons are referred to as layers with sedimentary or structural features that can be distinguished from the background sedimentary sequence. The main concern has been to identify event horizons whose relationships to earthquakes can be confidently demonstrated. Such event horizons are called seismites.

Appropriate criteria must be used to discriminate between 'normal' lacustrine sedimentation, earthquake-related sedimentary structures and other event features not usually associated with earthquake shaking. The Appendix gives a detailed description of late Pleistocene and Holocene event horizons, using macroscopic lithology, radiocarbon dating, pollen concentration, X-ray radiograms and tomograms. The contemporaneity of events in different boreholes of the same sedimentary basin and in different lake basins is the strongest argument for an earthquake origin, although not the only one.

The initial goal—to explore the potential of lake sediment investigations as a palaeoseismological tool in the region north of the Alps—was achieved during a drilling campaign in 1997–1998. A number of event horizons from two lakes in the Basle region, Seewen in northern Switzerland and Bergsee in southern Germany (Figs 1 and 2), have been identified and correlated using different dating techniques. Based on soft-sediment deformation characteristics and a comparison of these results from two sites, a palaeoseismic record for this region has been derived. Even though a precise characterization of pre-historic earthquakes in terms of magnitude and location has not been achieved, it can be shown that the investigated record of the maximum number of large earthquakes adds crucial constraints for earthquake hazard assessment.

2 SEISMICITY AND SEISMIC RISK IN THE BASLE REGION

The Basle region is one of higher seismicity in Switzerland, as shown by the instrumental and historical record dating back to 1000 AD (http://seismo.ethz.ch/products/catalogs/iecos, http://seismo.ethz.ch/products/catalogs/mecos/). Recent seismicity has been weak; the largest events of the last 20 years occurred in 1980 in Sierentz, in the Upper Rhine Graben NW of Basle, with a swarm culminating with the 1980 July 15, Sierentz $M_L = 4.4$ earthquake (Fig. 2). Recently, earthquake clusters have been recorded in the Jura Mountains near Läufelfingen (Fig. 2), around Basle and in the Dinkelberg NE of Basle. Most of these earthquakes are shallow, with hypocentral depths in the 5–15 km range, and only a few of them reach larger depths down to 24 km (Bonjer 1997).

The Basle earthquake of 1356 October 18, with a MSK epicentral intensity of IX–X, is the strongest historical earthquake north of the Alps (Mayer-Rosa & Cadiot 1979; Meyer *et al.* 1994). Based on the mapping of the destruction of medieval buildings (mainly fortresses and churches) the epicentre of the Basle earthquake has been located about 10 km south of Basle at the intersection of the Jura Mountains with the Upper Rhine Graben (Fig. 2). Another large historical earthquake mentioned in chronicles is the AD 1021 earthquake, whose location in the Basle area (and even its occurrence) remains questionable (Alexandre 1990). Recent archaeological evidence suggests that the Roman city of *Augusta Raurica* (Fig. 2) was destroyed in 250 ± 5 AD by an earthquake, as dated numismatically (Furger 1998; Gans 1999). So far, *Augusta Raurica* is the only ancient site providing evidence for this possible earthquake, mainly because additional Roman remains of this age are rare in the region.

A cumulative logarithmic frequency–magnitude distribution of the seismicity of the last 1000 yr in the greater Basle region has been constructed by converting the intensities given in the MECOS catalogue (http://seismo.ethz.ch/products/catalogs/mecos/) to magnitude, using the regression $M = I/2 + 1.8$ of Karnik (1969). With this regression, the AD 1356 earthquake is assigned a magnitude of 6.3. The logarithmic distribution shown in Fig. 3 displays a linear decay in the magnitude range $M_L = 4.3$–6.3 (Fig. 3); a fit is drawn using only the points corresponding to whole number intensity grades (V–VIII). The catalogue appears reasonably complete down to magnitude 4.5, but contains only two events with a magnitude exceeding 6 (AD 1021 and AD 1356), and of these two the existence of the AD 1021 event appears uncertain (Alexandre 1990). Assuming, as a working hypothesis, that the seismicity smaller than $M_L = 5.8$ is stationary, i.e. that events of this size will recur over longer time periods with the same magnitude–frequency distribution, we extrapolate the 1000 yr activity to a 10 000 yr period, to obtain the expected activity rates for the Holocene period (Fig. 3). For higher magnitudes we may expect different scenarios, leading to very different activity rate curves:

(A) the stationary seismicity hypothesis assumed in probabilistic hazard assessment would consider the occurrence of the two larger events (AD 1021 and AD 1356) as representative of the 1000 yr period with an expected occurrence of 20 such events over 10 000 yr, resulting in an unbounded linear Gutenberg–Richter decay (line A and the upper triangles in Fig. 3);

(B) a commonly used modification of the unbounded Gutenberg–Richter linear decay (Lomnitz-Adler & Lomnitz 1979; Young & Coppersmith 1985) would produce a curve truncated by a M_{max} obtained by adding a $0.5M$ grade to the largest observed event (line B and upper triangles in Fig. 3);

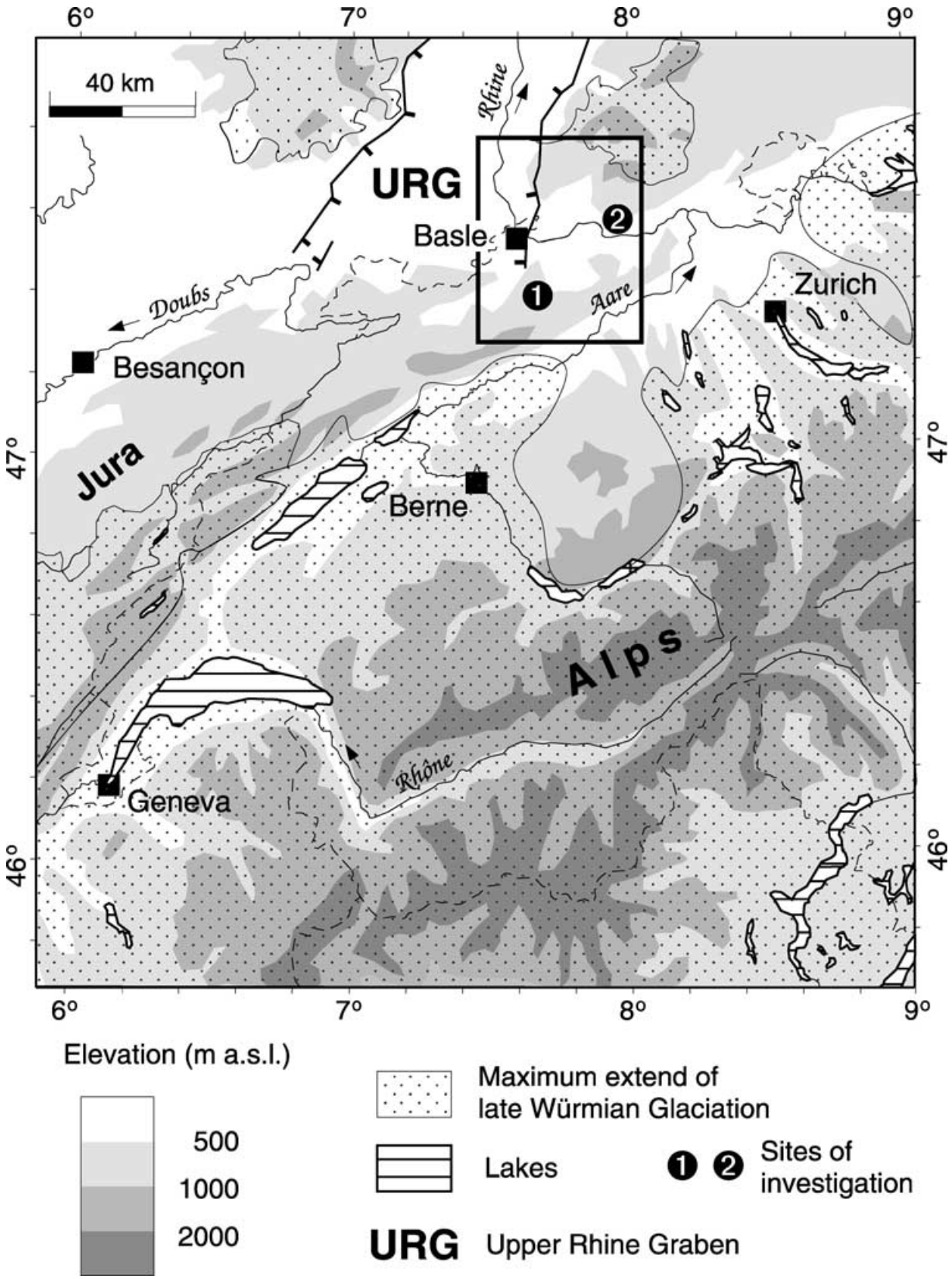

Figure 1. Topographic and drainage map of Switzerland and neighbouring countries, showing the extent of the late Würmian glaciation. The lakes in the Basle region (black frame) are shown as 1 and 2.

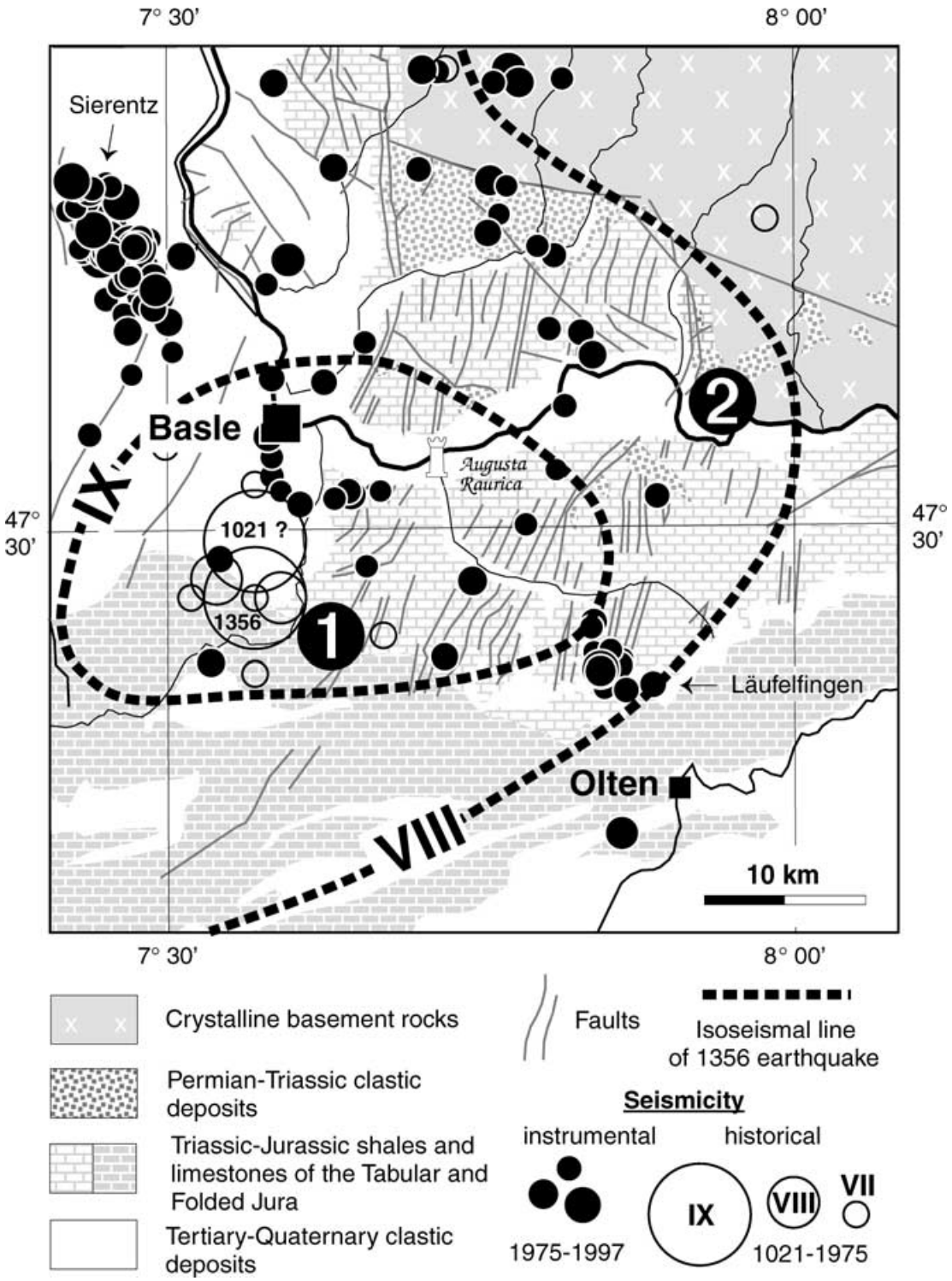

Figure 2. Geological map of the Basle region with instrumental and historical seismicity. Lake Seewen and Lake Bergsee are shown as 1 and 2. The isoseismal lines VIII and IX of the AD 1356 Basle earthquake are indicated.

(C) a more conservative scenario would eliminate the AD 1021 event as false (Alexandre 1990) and expect ten AD 1356-type events over 10 000 yr with a 0.25 increment for M_{max} (line C and the lower triangles in Fig. 3);

(D) a minimum scenario would accept the 1356 event as the only large earthquake expected over a 10 000 yr period (line D and the lower triangles in Fig. 3).

The corresponding activity rate curves for these four models are similar at low magnitudes, but very different at higher magnitudes. The difference is modest for the 475 yr return period commonly assumed in hazard mapping for seismic building codes (10 per cent non-exceedance probability in 50 yr), but becomes dominant for the higher return periods and low occurrence probabilities required for the design earthquakes of critical facilities. A palaeoseismological

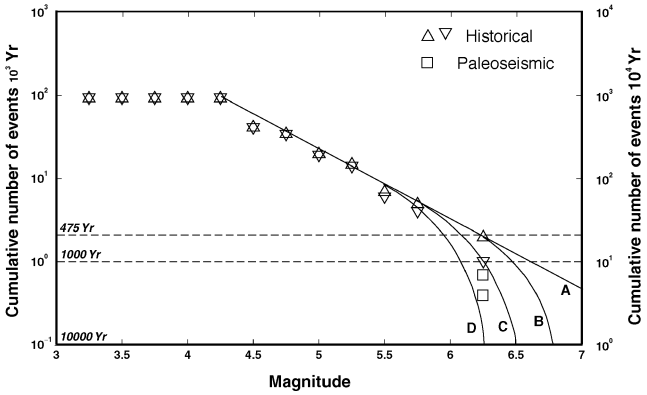

Figure 3. Frequency–magnitude diagram for the Basle region (as seen in Fig. 2) for a 1000 yr period (Sellami, personal communication). Magnitudes were converted from epicentral intensities following Karnik (1969).

record is needed to constrain these data and provide a realistic expectation of strong earthquakes for the Basle region. While we do not expect to obtain precise locations or sizes for pre-historical earthquakes just from lake sediment investigations, we intend to characterize the recurrence of strong earthquakes with sizes comparable to or larger than that of the AD 1356 Basle event.

3 GEOLOGICAL SETTING

The two lakes chosen for palaeoseismic investigations are the former lake at Seewen and the Bergsee. They are located 14 km to the SSE and 26 km to the east of Basle, respectively (Figs 1 and 2). The near-field isoseismal lines of the AD 1356 event (Fig. 2) show that both lakes are within a zone of MSK > VIII, which is approximately equivalent to a local $M_L > 5.5$ near-surface event.

The former Lake Seewen is located along the border of the Folded Jura to the south and the Tabular Jura to the north. It was artifically drained in the late 16th century AD (Haeberli *et al.* 1976; Becker *et al.* 2000). Upper Jurassic limestones are the dominant lithology in the surroundings of the former lake, which are locally karstified. The lake basin extends over a distance of 2.5 km and its maximum width is approximately 500 m (Fig. 4); its catchment area amounts to 18 km^2. The depth contours of the former lake basin indicate a maximum thickness of the sediment infill of 20–25 m. The deepest part of the lake basin is close to its western termination, where a gorge-like outlet was blocked by the Fulnau landslide at the end of the Pleistocene (12 500 BP, with BP being conventional radiocarbon ages before present).

The Bergsee is located close to Bad Säckingen in the southern foothills of the Black Forest at an altitude of 382 m a.s.l. Hercynian gneisses and granites are the dominant lithology in the surroundings of the lake. At its southern margin a patch of clastic Permian deposits is preserved. The Bergsee is 350 m long and about 250 m wide, with a maximum water depth of 13 m (Fig. 5). Originally, it was fed only by groundwater and run-off from the hilly terrain in the immediate vicinity. The natural catchment area amounts to 0.1 km^2 only. Before the water level was raised several times during the last 200 yr by damming the western outlet of the lake, the lake basin had a length of only 200 m and a width of 180 m. Bergsee is much older than Lake Seewen. It is part of a system of subglacial channels close to the margin of the former Rhine glacier, probably formed at the maximum stage of the Riss glaciation, some 130 000 BP (Metz 1980).

A prerequisite for small lakes to supply a complete sedimentary record for the Holocene and the latest Pleistocene is to be in locations that are bypassed by the major fluvial drainage channels and that do not experience rapid infilling resulting from large quantities of variable gravel-dominated sediment supply. With respect to this, both lakes—Seewen and Bergsee—are favourably positioned. They are situated outside of the major fluvial drainage channels of the rivers Rhine and Aare (Figs 1 and 2) and were not directly affected by glaciers during the Würmian maximum (Fig. 1). One major difference between the lakes is found in the surrounding geology. The catchment of former Lake Seewen (1 in Figs 1 and 2) is dominated by Mesozoic limestones and shales of the Tabular and Folded Jura Mountains, whereas for Bergsee (2 in Figs 1 and 2) granites, gneisses and Permian clastics prevail. Therefore, the initial expectation was that a clastic input in the lacustrine deposits of Bergsee is more likely than for Seewen, where chemical weathering and dissolution of limestones dominates.

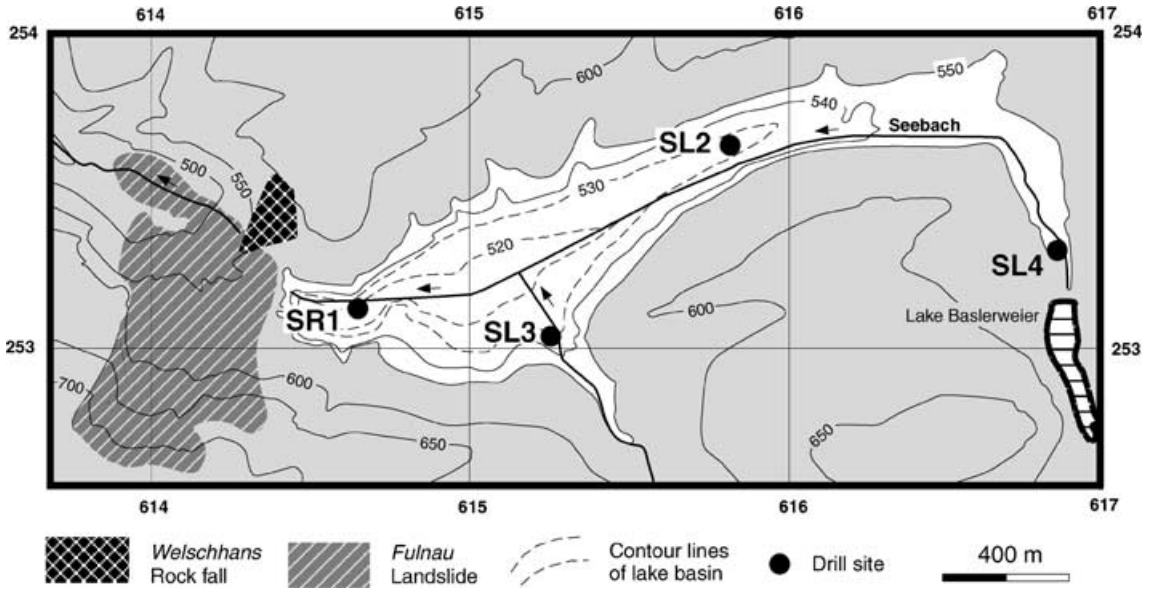

Figure 4. Topographic and bathymetric map of Lake Seewen showing the drill sites. The white area marks the maximum extent of Lake Seewen.

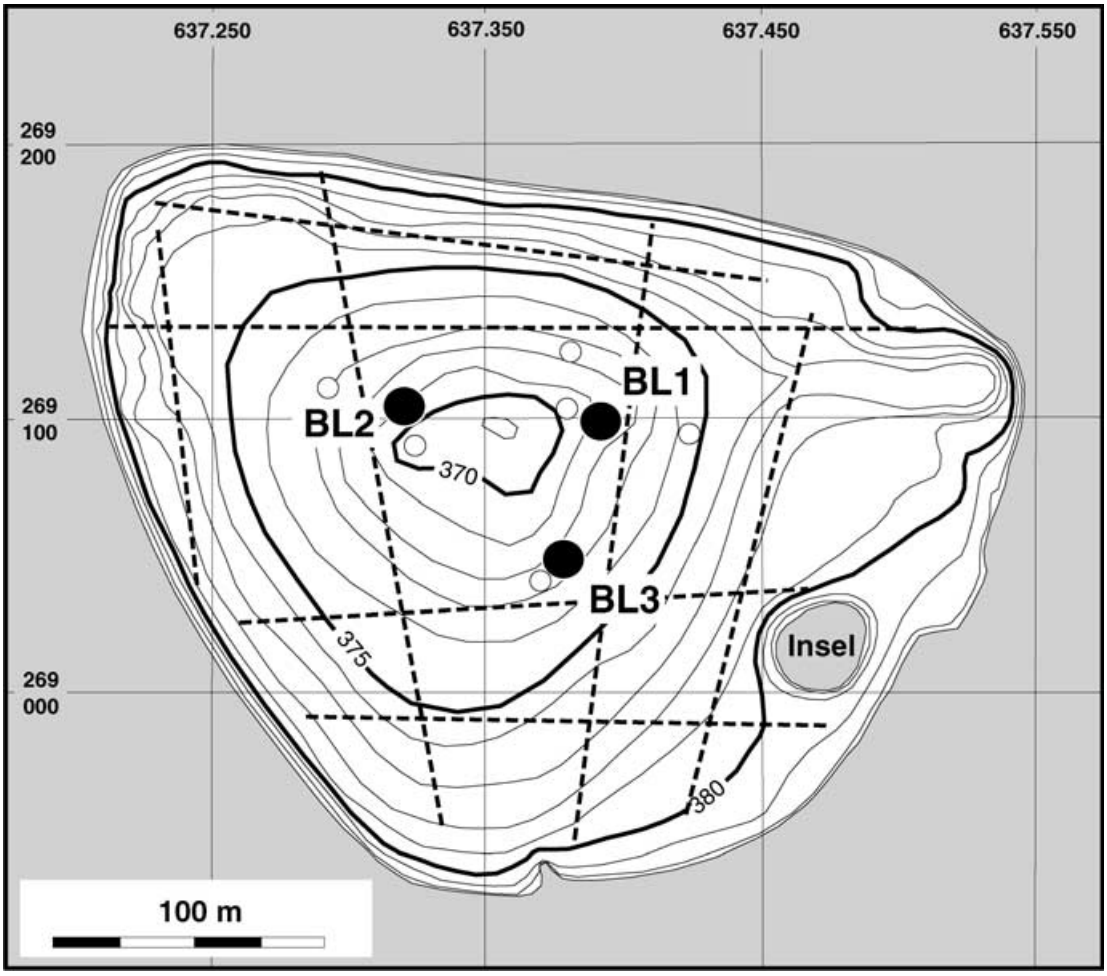

Figure 5. Bathymetric map of Bergsee with contour lines in metres a.s.l., showing positions of reflection seismic lines (broken line), short core (white circle) and Livingstone core drill sites (black dot).

4 METHODS

The methods applied on both lakes include seismic surveys, drillings, macroscopical descriptions of core samples, particle size analyses, radiocarbon datings, pollen analyses as well as X-ray radiography and X-ray tomography in the laboratory.

A refraction seismic survey using explosives was carried out along several lines in the western basin of Lake Seewen with a total length of 3460 m (Haeberli *et al.* 1976). Based on this survey the depth contours for the former lake basin could be drawn. In Bergsee a 3.5 kHz reflection seismic survey was carried out to obtain detailed structural information concerning the sedimentary basin infill and its thickness; because of the high gas content in the uppermost Holocene sediments, the penetration depth was restricted to the top 1.0–1.5 m and only in some isolated spots could we obtain information concerning the deeper sediments. Nowhere could the base of the lake basin be reached.

Drill cores were recovered by the use of ram coring and the Livingstone probe. The ram coring method was only used at the drill site at the deepest part of the basin of Lake Seewen (SR1). For the ram coring, a PVC liner within a casing was forced with a hammer, 1 m into the ground. The liner contains the core sample, which is now well protected. Liner and casing are overcored afterwards and recovered from the borehole with a winch. The ram core diameter was 100 mm. The Livingstone probe contains a piston at the tip of the core barrel (Merkt & Streif 1970). The barrel was forced into the ground, whilst the piston was held in position. After the Livingstone probe reached the final depth, the core barrel, containing the sediment core, was pulled off the borehole without any additional overcoring. The Livingstone drills have a core diameter of 80 mm in the uppermost 7 m, changing to 50 mm at depth in Lake Seewen and for Bergsee the core diameter changes from 80 mm in the uppermost 10–12 m to 50 mm at depth. In Lake Seewen boreholes were drilled to the base of the lake deposits at four sites, three of these were along the axis of the former lake and one at its southern margin (Fig. 4). Three boreholes were drilled at 2–3 m distance at sites SL2 (SL2.1–SL2.3) and SL3 (SL3.1–SL3.3), and only one borehole was drilled in SR1 and SL4. For Bergsee the drill sites were close to the centre of the lake (Fig. 5). Two boreholes were drilled at 2–3 m distance at sites BL1 (BL1.1, BL1.2) and BL2 (BL2.1, BL2.2), and only one borehole was drilled at BL3.

After careful splitting of the drill cores parallel to the long core axes using a plate or a string wire, the drill cores were described macroscopically and photographed. One half was taken for sampling and the other half for X-ray investigations. Samples were taken for particle size analyses, pollen analyses and radiocarbon datings. The particle size analyses, using standard methods, were carried out at the Geographical Institutes of the Universities of Basle and

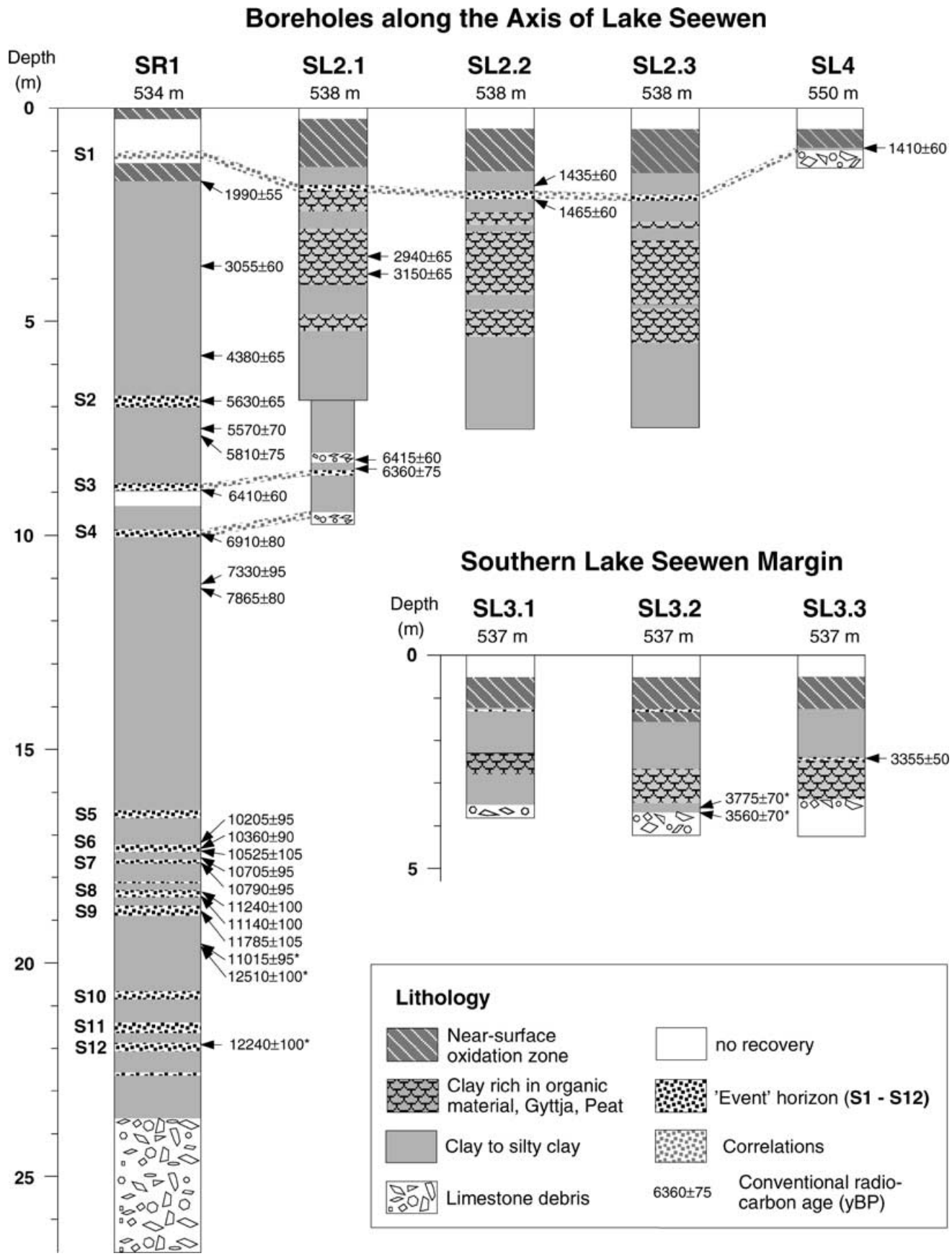

Figure 6. Simplified lithological profiles of the boreholes in Lake Seewen, indicating radiocarbon ages and event horizons S1–S12. Asterisks mark critical radiocarbon dates.

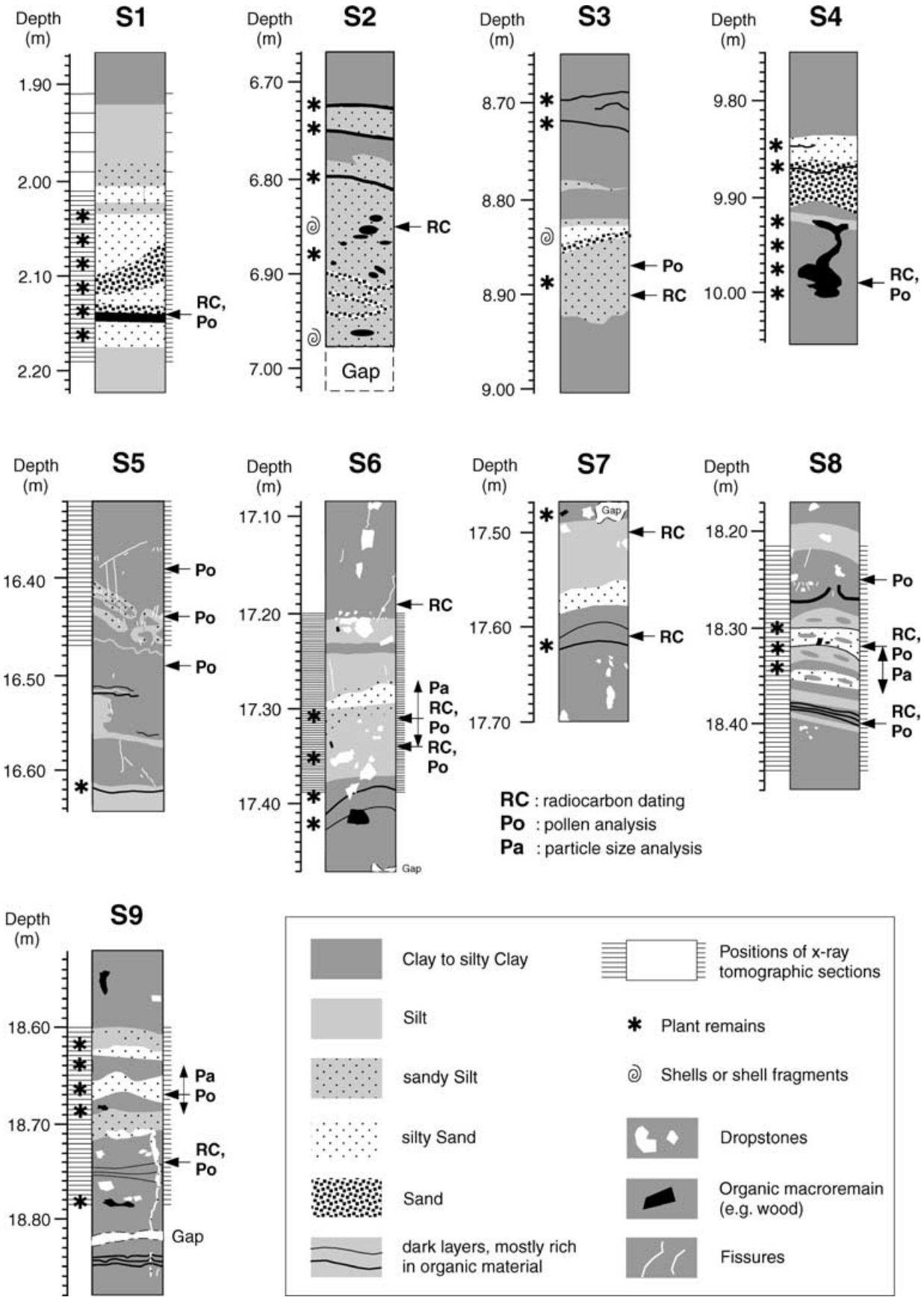

Figure 7. Lithological description of event horizons S1–S9 from Lake Seewen. Details are given in the Appendix. Sampling sites for radiocarbon dating, pollen and particle size analyses are indicated.

Figure 8. Photograph showing the upper part of event horizon S5 with the deformed silt and silty sand layers at Seewen borehole SR1. The core diametre is 100 mm.

Zurich. The pollen analyses were carried out by Roger Perret and Guiseppe Sampietro at the Geographical Institut of the University of Zurich.

Altogether 43 samples from Lake Seewen and Bergsee were taken and prepared for accelerator mass spectrometry (AMS) radiocarbon dating. Plant fibres, wood and charcoal particles, as well as macroremains were picked out by hand. Dating is restricted to terrestrial plant material. After a standard acid–alkali–acid pre-treatment (AAA), the samples were dried and combusted in quartz tubes for further processing. Samples containing dispersed carbon material also required AAA-pre-treatment, whereby, after each step, material was centrifuged. After pre-treatment, the CO_2 obtained was cracked to graphite. The preparation and pre-treatment of the samples for radiocarbon dating was carried out at the ^{14}C-laboratory of the Department of Geography at the University of Zurich. The AMS with the tandem accelerator from the Institute of Particle Physics at the ETH-Hönggerberg was used for dating. The results of the 31 ^{14}C-datings from Lake Seewen are given in Becker *et al.* (2000). The results of the remaining 12 samples from Bergsee are given in Table 2. The calibrated values were calculated using the programs 'CalibETH' and 'OxCal'.

X-ray radiography and X-ray tomography were carried out on half-core samples at the Swiss Federal Laboratories for Materials Testing and Research (EMPA) in Dübendorf, Switzerland. Technical details are given in Becker *et al.* (2000) and Flisch & Becker (2002).

5 FORMER LAKE SEEWEN

5.1 Observation

Simplified lithological profiles of the eight boreholes from four drill sites in former Lake Seewen are shown in Fig. 6. The base of the lacustrine sequence is marked by debris (i.e. SR1) or talus (SL4). The most common lake deposit is a sticky silty clay, which is slightly oxidized in the uppermost 1–1.5 m. The drill sites SL2 and SL3 show some gyttja (organic-rich shallow-water lake deposit) and peaty layers. Dropstones in the lower (Pleistocene) section of SR1 are common.

The lacustrine sequence shows intercalations of thin more coarse-grained silty-sandy layers, which can be based on radiocarbon datings partly correlated between different boreholes along the long axis of Lake Seewen (Fig. 6). These event horizons, which share structural or sedimentary features distinguishable from the uniform silty clay background sedimentary sequence, are numbered from top to bottom (S1–S12). In the Appendix a detailed description based on the (macroscopic) lithology, radiocarbon ages, pollen concentration, X-ray radiograms and tomograms is given of the nine event horizons S1–S9 shown in Fig. 7. The deepest three event horizons, S10–S12, are not reported here in detail because they are difficult to distinguish from the background sedimentation in the small landslide-dammed lake formed shortly after impounding. Of the 12 event horizons shown in Fig. 6, S2 and all event horizons older than S4 can only be seen in borehole SR1. S1 cannot be seen in SR1 because of a lack of recovery at this shallow depth, however, it is well developed in the cores of site SL2 and correlates with the onset of lacustrine sedimentation at site SL4. S3 is recognized in SR1 and in SL2.1, and S4 in SR1 correlates with the onset above debris of lacustrine sedimentation at site SL2.1 (Fig. 6).

5.2 Interpretation

5.2.1 Event horizons of non-seismic origin

In the deep borehole SR1, event horizons appear to be arranged in three depth intervals: 6.7–10.1, 16.3–19.0 and 20.6–22.6 m. Based on radiocarbon ages and palynostratigraphic evidence, the deepest two intervals seem to coincide with two periods of climatic deterioration at the end of the Pleistocene, the Older Dryas and the Younger Dryas (Becker *et al.* 2000). Similarly, the upper depth interval seems to correspond with the transition from the Mesolithic to the Neolithic ages, i.e. the onset of agriculture in the Basle region (Probst 1991; Strahm 1997). Long-term environmental changes caused by climate and by human impact on vegetation and drainage such as forest clearance, floods and slope failures may have caused some of the event horizons seen in former Lake Seewen.

Since significant clastic sedimentation can be expected in the tributary-controlled basin of Lake Seewen, event horizons caused by extraordinary floods can be expected. A clear indication for such flood deposits in the sedimentary record is a decrease of grain size and overall layer thickness from proximal to distal positions in a lake basin (Sturm *et al.* 1995). Furthermore, plant chaff is very common in such flood deposits. The clearest indication of a flood event seen in Lake Seewen is found in event horizon S3 where a coarse-grained layer in SL2.1 proximal to the former Seebach mouth can be correlated with distal fine-grained sediments of the same age

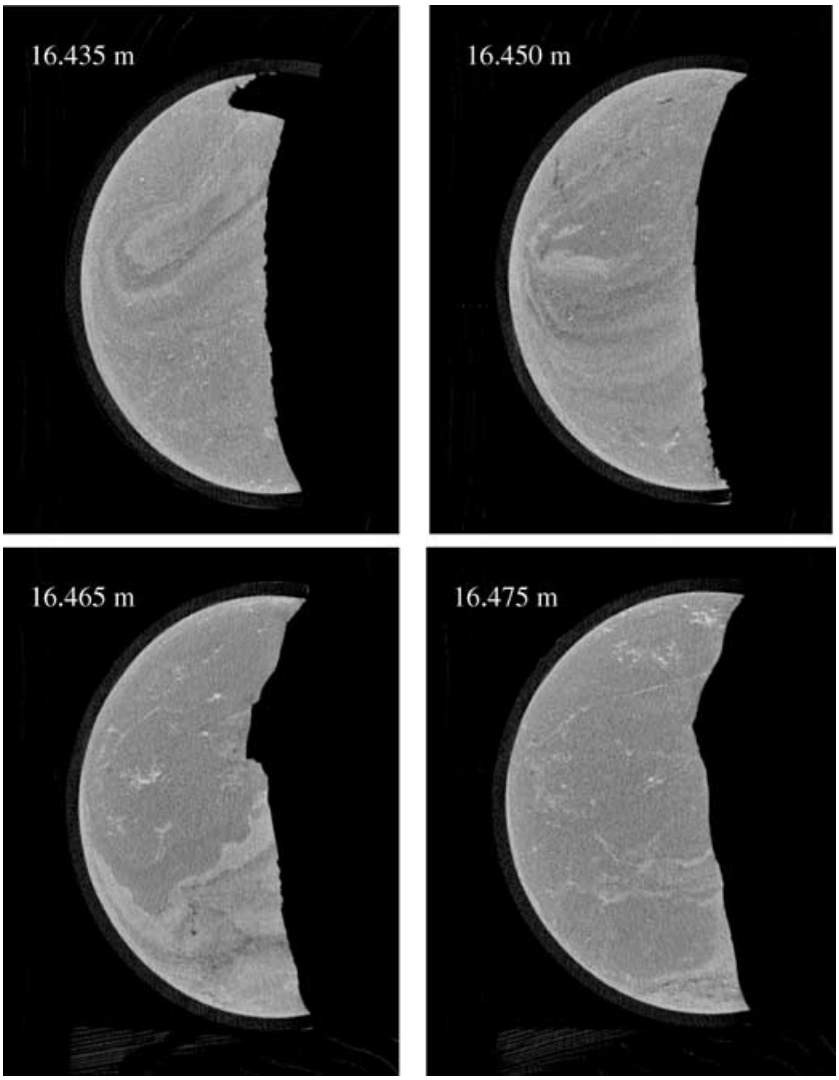

Figure 9. Four X-ray tomographic sections through event horizon S5 in borehole SR1 between 16.435 and 16.475 m depth, showing two cuts through an updoming with concentric layering (16.435 and 16.450 m), followed by a section showing a very clear, undulating boundary between clay-rich and more silty sediments and first small fractures (16.465 m). In 16.475 m four fractures are visible. The four sections are cuts perpendicular to the long axis of a half-core.

in SR1 (Figs 4 and 6). Also S1, S4, S6–S9 contain evidence of floods. Event horizon S2, which can be seen only in SR1, shows different conditions, favouring reworking processes close to the former shore line at a time of a low lake level stand instead of a flood event.

In contrast to flood deposits the grain size of slide and slump deposits does not change much across the lake basin and the overall thickness is largest at distal basin sites (Sturm *et al.* 1995). In the case of slump deposits a high amount of plant remains would not usually be expected, which is more probably a result of vigorous surface run-off in the surroundings of the lake during floods. So far no signs of slides and slumps within the lake basin or its surroundings could be seen, which may have influenced the local drainage system, other than the Fulnau landslide, which caused the impounding of the lake.

5.2.2 Seismites in Lake Seewen

Pre-historic earthquakes can be detected based on different kinds of evidence. Primary evidence is given by the co-seismic offset along a seismogenic fault creating a fault-scarp at the Earth's surface. Secondary earthquake evidence is related to *in situ* deformation features without significant lateral movements such as soft-sediment deformation structures and fractures in lake deposits. Tertiary evidence can be seen in mass movements triggered by earthquakes, such as turbidity currents, slides, slumps and rockfalls. Even fourth-order earthquake evidence is possible, such as flood deposits in a lake caused by the overtopping and collapse of an earthquake-triggered rockfall dam blocking a river channel. Neither first nor fourth-order evidence could be observed in Lake Seewen and its vicinity. Slope instabilities are frequent in the Seewen area; however, they seem to be of no significance for the deformation features seen in the lake deposits. Thus, only *in situ* deformation features, i.e. secondary evidence, may point to the occurrence of strong pre-historic earthquakes in the Seewen area. Event horizons, which can be related to earthquakes are called seismites.

The sediments in the Lake Seewen are not generally favourable for earthquake-triggered liquefaction because of the high silt and clay content. However, some of the event horizons with a higher content of coarse silt and sand may have been susceptible for liquefaction during earthquake shaking causing soft-sediment deformations. In the case of slightly consolidated cohesive sediments,

Figure 10. X-ray radiogram showing the trace of the small sand dyke of event horizon S9. The scale is in centimetres.

fracturing could be a possible mode of seismically induced failure. Deformation features in an environment of high sedimentation rates can be generated owing to normal sedimentary processes related to density instabilities (e.g. load casts, ball-and-pillow structures) or de-watering (sand dykes, water-escape structures such as dish structures), whereas in an environment with low sedimentation rates such features are more unlikely, demanding unusual circumstances such as earthquake shaking. High amounts of plant remains in the sediments, such as plant chaff, may point to rapid sedimentation. Although shell fragments may indicate rapid sedimentation, they may also point to re-working processes such as for instance wave action, which can also generate liquefaction structures. High pollen concentration in lake deposits indicates either a high primary pollen production, a reduced sedimentation rate or a re-sedimentation of pollen grains after the resuspension of already deposited sediments, possibly caused by earthquake shaking. Rapidly deposited sandy layers may be the source for liquefaction at a later stage, by initiating sand injections such as sand dykes into more cohesive caprocks and may even cause sand ejections at the lake bottom. In general, deformation features in a low sedimentation rate environment are more likely to be related to earthquake shaking, whereas all deformation structures related to gravity instabilities in a high sedimentation rate environment are more likely to be related to normal sedimentary processes and only those indicating an injection into cohesive caprocks are more likely to be related to earthquakes.

The clearest indications for a seismite, i.e. an earthquake triggered event horizon, are found in S5 (Appendix, Fig. 7, Table 1), showing small-scale layer folding and doming, dewatering features (Fig. 8) and fractures (Fig. 9) within a background of slow sedimentation. The breaching and doming of the two deformed layers could have taken place only in soft-sediment conditions close to the water–sediment interface and the apparently simultaneous development of fractures associated with the silty deformed layers can be explained by strain hardening of slightly denser sediment during shaking (Davenport 1993). The fractures in the deeper part of S5 and the upper part of S6 (Fig. 7) are more likely to be the results of a brittle failure process in more consolidated and cohesive clay-rich deposits. Because these fractures in S6 lie only 50 cm below S5, they may well be part of the same seismic event.

Event horizons S8 and S9 exhibit other features that are attributable to loading conditions associated with rapid sedimentation and/or earthquake shaking, such as layer disruption (Fig. 7) owing to dewatering, clay clasts and a small sand dyke (Fig. 10). In the case of event horizon S2 reworking processes close to the former shore line are favoured for the observed cross-bedding such as structures, patches of organic material and shell fragments, however, a seismic origin cannot be fully excluded.

6 BERGSEE

6.1 Observation

Simplified lithological profiles of the five boreholes from three drill sites in Bergsee are shown in Fig. 11. Nowhere could the base of the lacustrine sequence be reached. Lithologically the cores can be clearly divided into a Holocene–latest Pleistocene section rich in dark red-brown to black organic material (mainly gyttja, with peaty gyttja or even peat in the uppermost section), and an older Pleistocene silty clay section (Fig. 11), showing a maximum AMS radiocarbon age of 29 110 $\pm$ 280 BP (Lascaux-UIa or Denekamp Interstadial based on palynostratigraphy) in the deepest borehole BL3.1. The details concerning the radiocarbon datings are given in Table 2. Gyttja is an elastic jelly-like soft lacustrine deposit, which originates from remains of plants and animals (Larsson 1990), and is very homogeneous in Bergsee. Clastic input within the gyttja section is low, concentrated in very thin silty-sandy layers, sand pockets and lumps or dispersed single sand grains (mainly feldspar). An exception can be seen in the boreholes BL1.1, BL1.2 and BL3.1 just above the base of the gyttja where sandy silt is concentrated in discontinuous layers. This is the only sedimentary event horizon (B5) seen in Bergsee. Altogether, five event horizons (B1–B5) have

Table 1. Some characteristics of event horizons S1–S9 in Seewen. Abbreviations: S, sand; s, sandy; U, silt; u, silty; C, clay; c, clayey; ++, strong; +, elevated; o, background; −, low; −−, weak; ?, not known in detail.

	Event horizons in Lake Seewen								
	S1	S2	S3	S4	S5	S6	S7	S8	S9
Sediment type	S–sU	(S)–sU	S–sU	S–uS	sU–sC	uS–U	uS–U	uS–uC	uS–uC
Sedimentation rate	++	(o)	+	+	−−	−	o	++	+
Plant remains	++	+	+	++	−−	+	o	+	+
Shell fragments	−	+	+	−	−	−	−	−	−
Pollen concentration	?	?	o	−	++	o	?	o	o
Soft–deformations	−	−	−	−	++	−	−	+	+
Fissures	−	?	?	?	++	+	−	+	−
Dykes	−	?	?	?	−	−	−	−	+

Table 2. Summary of radiocarbon age datings from Bergsee. For the calibration CalibETH and OxCal (marked with ∗) were used. The measurement marked with ∗∗ is out of the calibration range.

Drill hole	Lab code [UZ-]	Depth (m)	Convent. ^{14}C age (BP)	Dendro-calibrated dates from cumulative probability [BC/AD]		δ^{13}C (per mille)	Material
				1σ-range	2σ-range		
BL1.1	4251	4.01	2995 ± 50	1298 BC–1134 BC	1376 BC–1049 BC	−22.8	Plant fibres
	4252	7.36	6970 ± 60	5886 BC–5741 BC	5943 BC–5693 BC	−19.4	Disp. material
∗	4253	12.79	11 290 ± 80	11 460 BC–11 200 BC	11 550 BC–11 050 BC	−25.8	Disp. material
BL1.2∗	4250	13.06	11 340 ± 80	11 470 BC–11 220 BC	11 550 BC–11 050 BC	−26.8	Disp. material
BL2.1	4247	3.01	3360 ± 50	1695 BC–1556 BC	1747 BC–1525 BC	−21.5	Disp. material
	4248	5.30	5175 ± 55	4042 BC–3864 BC	4203 BC–3816 BC	−23.3	Disp. material
	4249	5.63	5595 ± 60	4487 BC–4373 BC	4553 BC–4342 BC	−23.1	Disp. material
BL2.2	4246	2.86	3190 ± 50	1503 BC–1413 BC	1577 BC–1329 BC	−19.0	Disp. material
SL3.1	4242	3.22	3220 ± 50	1526 BC–1435 BC	1607 BC–1399 BC	−18.5	Plant fibres
	4243	8.70	8515 ± 70	7577 BC–7480 BC	7693 BC–7398 BC	−20.8	Disp. material
∗	4243	12.55	11 700 ± 80	11 880 BC–11 520 BC	12 200 BC–11 300 BC	−21.1	Disp. material
∗∗	4245	20.46	29 110 ± 280	(27 450 BC–26 850 BC)	(27 800 BC–26 600 BC)	−21.1	Disp. material

been identified so far in the Bergsee, as described in the Appendix. Four (B1–B4) of the event horizons are characterized by fracturing (Fig. 12) and the fifth (B5) exhibits soft-sediment structures. Some fractures show blue, brown and white mineral coatings as can be seen in the sites BL1 and BL3 at a depth of 10 m or more. In the case of the blue coatings a thin veneer of vivianite is most likely, because vivianite is a common mineral in the gyttja deposits of Bergsee, which generally occurs in large patches within the sediment. Some fractures contain single sand grains (most likely feldspar). In some parts the core samples are irregularly broken showing small cracks.

In case of fracturing, the correlation of the event horizons amongst the different boreholes is based on depth–age conversions based on radiocarbon datings or direct radiocarbon datings on samples just above the minimum depth where fractures could still be observed. The correlation of event B5 is based on radiocarbon datings and tephrastratigraphy (Laacher See Tephra: LST). As can be seen in Fig. 11 fracturing is not randomly scattered but seems to be concentrated in certain depths in the different boreholes. B1 can be seen in all boreholes but BL2.1 can only be seen at depths between 3 and 4 m. In BL2.1 only sand pockets and lumps of silt can be seen at this depth, whereas the cracks and fractures in BL1.1 and BL1.2 may be at least partly artificial. B2 can only be seen in site BL1 and the borehole BL2.1, whereas B3 is only developed in site BL1. B4 can be seen in all sites, however, in BL1.2 only some tiny silt layers and sand pockets can be seen in the depth interval correlating with the fractures in the remaining drill sites. B5 could be found in all boreholes, which reached the depth of the event horizon.

6.2 Interpretation

The low clastic input is related to the tiny catchment area of the Bergsee, i.e. the tributary flow has not been sufficient to create significant clastic layers. The only exception is event horizon B5, where some of the clastic material comes from the LST event and some from the surroundings of the lake as run-off. The origin of the sand pockets in the gyttja is not clear in any case. At least it has been observed that sand accumulations are sometimes related to beechnuts. One possibility is that sand became stuck to beechnuts before they were deposited in the lake. In the lake environment the organic material decomposed and the sand accumulation was left creating a sand pocket. Thus, it is not very likely to assume a sedimentary or even seismic origin for the generation of the sand pockets. Therefore, fractures seem to be the most prominent expression for earthquake shaking in such homogenous organic deposits such as the gyttja from Bergsee. Fractures have been considered to be natural if the fracture surfaces were coated by minerals. Another argument for naturally generated fractures is a dip larger than 30°, whereas in all cases of horizontal or close to horizontal fractures, core expansion or bending owing to core squeezing out the core tube may be responsible for fracturing. The observation of only a few sand grains in cracks may indicate water escape, which transported

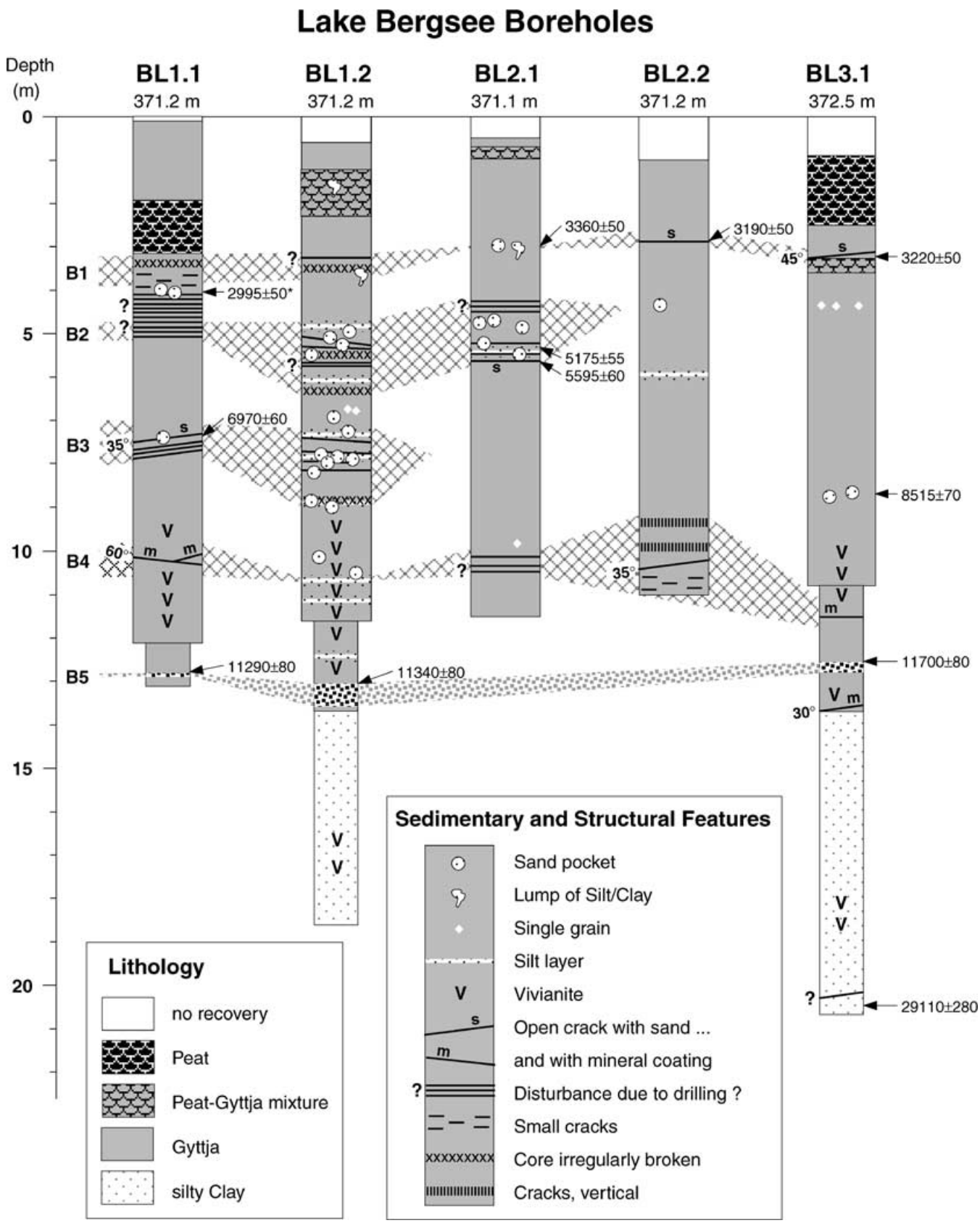

Figure 11. Lithological profiles of the five boreholes from Bergsee, showing radiocarbon ages (BP) and the event horizons B1–B5.

some rare mineral-particles in the fracture void. However, in the case of horizontal fractures sand grains may simply have nucleated tension cracks during core expansion. The clearest evidence for natural fracturing can be seen in B4 with three fractures in two boreholes showing mineral coating (Fig. 12) and one fracture dipping at 35°. In the case of B1 in two boreholes of two sites cracks with some sand fill can be observed; one crack shows a dip of 45°, the other one is partly horizontal. In the case of B2 only one short crack contains an angular feldspar grain and in the case of B3, again, only one crack shows some sand. However, in B3 it appears that the crack has been initiated by a sand pocket, and therefore sand injection can be largely excluded.

6.2.1 Event horizons of non-seismic origin

We have only weak positive evidence for natural fracturing in the cases of the event horizons B2 and B3. Furthermore, fracturing related to B3 has been seen only in one site and nothing was observed in the other sites. Although we do not have evidence against a seismic origin for the observed deformation features, we believe that the evidence is not sufficient for a palaeoseismological interpretation.

6.2.2 Seismites in Bergsee

As in the case of Lake Seewen, Bergsee also exhibits structures that can only be interpreted as secondary earthquake evidence, i.e. *in situ* deformation features. B1, B4 and B5 display characteristics, which are not purely sedimentary or syn- and post-sample recovery structures. The clearest evidence for natural fracturing is seen in B4 with three fractures in two different drill sites showing mineral coating as well as a 35°-dipping fracture in the third site. Also, in BL2.1 some fracturing at a depth of 10 m could be observed, although only with a possible natural origin. BL1.2 does not show any fracturing, which could be related to B4. B1 is developed in two sites, in both cases with cracks containing some sand fill. In the third site, the origin of the fractures is not sure. However, fracturing can be seen at approximately the same depth in four of five boreholes. If fracturing can be triggered by earthquake shaking in very homogeneous jelly-like gyttja, then B1 and B4 are good candidates for seismites.

B5 has a number of features, which suggest syn-sedimentary modifications by natural processes, showing layers, which are interrupted and folded, and partly vertically connected. Sand and silt is locally enriched in diffuse sand lumps. Furthermore, if the sediments in B5 were deformed very close to the sediment–water interface by earthquake shaking, then fractures could have been generated in the deeper, more consolidated sediments (Seilacher 1969). Therefore, fracture observed in BL3.1 at 13.60 m depth could be the result of the shaking event that caused the soft-sediment deformation features in event horizon B5.

7 TIMING OF SEISMITES FROM LAKE SEEWEN AND BERGSEE

In the case of sedimentary event horizons, the earliest possible dates for the events causing the disturbances seen in the event horizons are determined either directly from age datings, or were estimated by interpolation from the depth–age relationship of the undisturbed material deposited immediately above the event horizon, assuming continuous sedimentation. For fracture events alone, estimates of dates using this principle may not give the actual age of the event because the conditions for fracturing require their formation in sediments, which are at some distance below the water–sediment interface. This is to allow for some consolidation to take place. Events creating fractures could be as much as 1000 or several thousand years younger than the fractured sediments, depending on the sedimentation rate and the degree of consolidation. Hence, a window of possible event occurrence, based on the age of the event horizon is necessary to define. Based on the drill core investigation it could

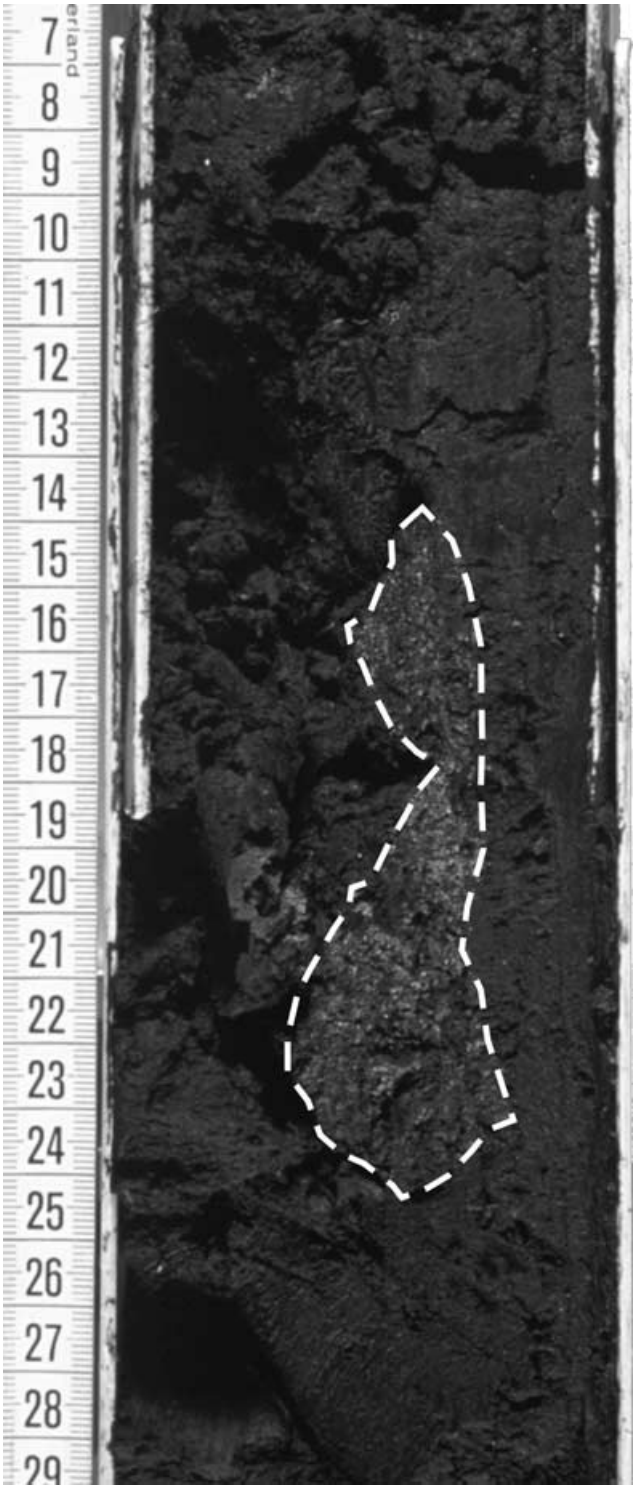

Figure 12. Photograph showing partly exposed fracture (fracture surface surrounded by broken line) with blue and white mineral coating (vivianite) of event horizon B4 in Bergsee borehole BL1.1.

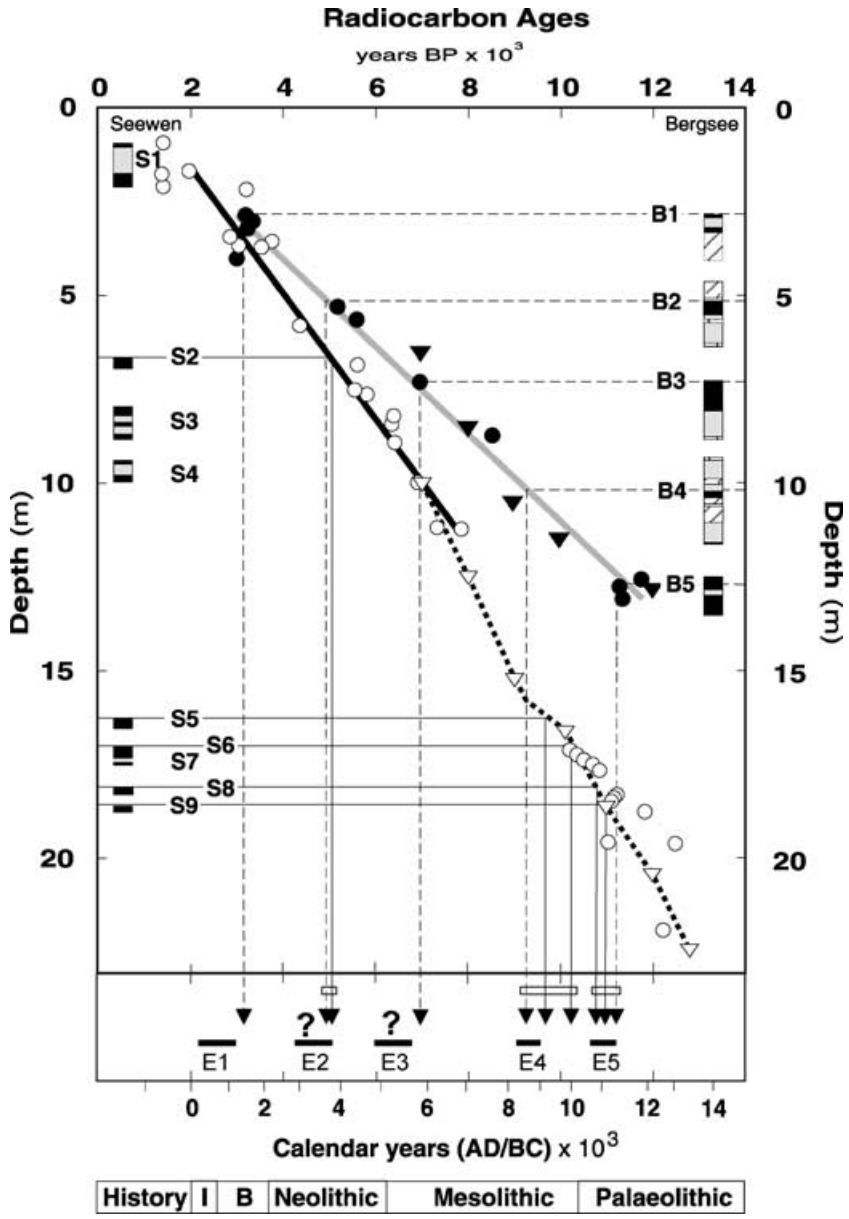

Figure 13. Correlation diagram of depth of event horizons S1–S9 from former Lake Seewen and B1–B5 from Bergsee versus radiocarbon ages and calendar years. Depth intervals for event horizons for Seewen are marked on the left-hand side, for Bergsee on the right. Black sections mark the position of the event horizons in the different boreholes below ground surface, grey mark their depth range, and hatched sections are of unsure origin. White and black dots mark radiocarbon ages, white and black triangles mark palynostratigraphic ages. White are from Seewen and black are from Bergsee. The black lines in the lower part of the diagram indicate the time intervals of the possible earthquake events E1–E5. The calibration of radiocarbon ages to calendar years is after Stuiver *et al.* (1998). In the archaeological timescale the abbreviations I refer to Iron Age and B to Bronze Age.

be possible that a gyttja from Bergsee at a depth of approximately 1 m is already stiff enough to suffer fracturing during earthquake shaking. A weak indication that this might be true can be seen in the possible relationship between event horizon B5 and the fracture below B5 in BL3.1.

The depth–age relationships for the sediments in both lakes using the results of extensive radiocarbon datings given in Figs 6 and 11 and Table 2 are shown in Fig. 13. For the deepest borehole in Lake Seewen (SR1) palynostratigraphic evidence has also been used to establish the depth–age relationship, especially for the depth interval between 11 and 17 m, where radiocarbon dates could not be obtained (Becker *et al.* 2000). For Bergsee only radiocarbon dates have been used, however, preliminary palynostratigraphic age determinations have been included in Fig. 13 for comparison. In Fig. 13 the total depth range of each event horizon for all drill sites in Lake Seewen is marked on the left-hand side, and those of Bergsee on the right-hand side. Uncertain events in Bergsee are hatched while grey sections indicate depth intervals in the different boreholes where the different event horizons were not detected. Radiocarbon and palynostratigraphic age determinations for the lakes Seewen and Bergsee are shown with white and black symbols, respectively.

In Bergsee the average sedimentation rate is of the order of 1.0 mm yr^{-1} (yr is the calendar year) for most of the Holocene and the latest Pleistocene, when not considering compaction. Compaction, however, is low and does not exceed 4.5 per cent at a depth of 11.3 m. In Lake Seewen, the average sedimentation rate is about 1.4 mm yr^{-1}

in the uppermost 10 m of sediments and slightly higher, at about 1.9 mm yr^{-1} down to a depth of 22 m. Compared with Bergsee the compaction of the clayey sediments in Seewen is higher; however, it has not yet been determined accurately. Based on the well-defined average sedimentation rates, an accurate correlation and age determination of event horizons is possible even in cases where no direct dating of single event horizons was possible.

Event 1. The event horizon B1 is weakly developed but it is seen at all drill sites in Bergsee. The youngest sediments containing fractures have a radiocarbon age of 3190 ± 50 BP (Fig. 11, Table 2), corresponding to a 1σ age in calendar years between 1503–1423 BC. Since an earthquake causing the fracturing must be younger, as explained above, a window of possible occurrence for this event has been assigned in the period 2170–3020 BP [∼180–1160 BC]. No evidence for a corresponding event has been found in the Seewen sediments.

Events 2–3. The evidence for these two events is only tentative: event 2 corresponds to the event horizons S2 and B2, event 3 to the event horizon B3. All of these event horizons have sedimentary and structural characteristics, which allow them to be identified in the sedimentary record, however, these characteristics are not sufficient to identify these event horizons as being earthquake related. In Fig. 13 the event horizons are indicated as possible earthquake events pending further drilling investigations, with windows of possible event occurrence at 2900–3850 and 4870–5660 BC.

Event 4. The event horizons that could most convincingly be related to a single earthquake event are S5 in Seewen and B4 in Bergsee (Fig. 13). This event is probably also responsible for the fractures in S6 which are only 50–60 cm deeper than S5 (Fig. 7). The soft-sediment deformation features seen in S5 indicate that deformation took place close to but not directly at the sediment–water interface. This is because the sediments need to be capable of producing fractures. Dating of the S5 event horizon is difficult because datable organic material is missing in the overlying younger sediments. Our estimate is therefore based primarily on palynostratigraphic evidence. In Bergsee, the most convincing fractures possibly caused by an earthquake occur in borehole BL1.1 at a depth of 10.18–10.32 m (Fig. 12). Assuming that the two event horizons B4 and S5 and the fractures in S6 can be explained by the same earthquake, and taking the fractures in BL1.1 as the youngest with the earliest possible date for the event (9550 BP), then we can give a window for the event occurrence between 8260 and 9040 BC.

Event 5. B5 in Bergsee is a sedimentary event horizon with soft-sediment deformation features. The fracture seen below B5 in borehole BL3.1 may be an additional indicator of an earthquake origin for the soft-sediment deformation features seen further up in B5. If this is true, then the soft-sediment structures must have been generated close to the sediment surface and the age is well constrained from the youngest date of the sediments immediately above B5, at 11 290 ± 80 BP. Event horizons S8 and S9 in Seewen show weak but clear deformation features. Event horizon S8 contains clay clasts, a small discontinuous layer (dewatering structure) and tiny fractures, with a radiocarbon age at 18.32 m of 11 240 ± 100 BP. Because the ages of events B5 and S8 are similar, they might be of the same origin. S9 contains a small sand dyke occurring just after the radiocarbon date of 11 785 ± 105 BP, providing an alternative correlation with B5 in Bergsee. A window of possible occurrence for a single earthquake event causing the event horizons B5 and S8 or B5 and S9, respectively, could then be identified tentatively at 10 720–11 200 BC.

8 CONCLUSIONS

The detailed investigations of the Holocene and late-Pleistocene sediments in Bergsee and Seewen allow a number of event horizons, which disrupt a very uniform sedimentary record in both lakes, to be identified. Some of the event horizons show features that point to an earthquake origin. Such event horizons are called seismites. Radiometric and palynostratigraphic dating allow one to correlate these seismites. Five time windows for possible earthquake events (E1–E5) in the last 12 000 yr at 180–1160 BC, 2900–3850 BC, 4870–5660 BC, 8260–9040 BC and 10 720–11 200 BC could be identified. Of these, the most convincing are E4 and E5. Although it is seen only in Bergsee, E1 appears to be earthquake triggered.

It is known from many palaeoseismological investigations that there is a magnitude threshold at which surface-faulting, liquefaction and soft-sediment deformation as well as slope-instabilities will be triggered by earthquakes. This threshold is about $M = 5.5$ for a local event (Davenport 1994; Keefer 1984; Wells & Coppersmith 1994), corresponding to a local intensity of MSK VIII in Switzerland (Rüttener 1995). Both lakes are located within the intensity VIII area of the AD 1356 Basle earthquake, for which the probable epicentre was within 10 km of Seewen and about 30 km from Bergsee (Fig. 2). Using an attenuation equation for MSK intensities for the Swiss Alpine foreland for shallow earthquakes, an earthquake anywhere in the Basle area with a magnitude equal to or larger than the AD 1356 event could explain the event horizons of supposed earthquake origin correlated in both lakes. Available data do not allow us to constrain the event size and location and we refer to a general 'AD 1356 Basle-type' event, implying an event with location and size comparable to that of the AD 1356 Basle earthquake. The event stratigraphy in Seewen and Bergsee seems to be consistent with the occurrence of 3–5 AD 1356-type earthquakes in the Basle area in the period 0–11 000 yr BC.

The investigations in the two lakes did not provide evidence for events in the historical period. This is a result of the influence of lake drainage, agriculture and unfavourable peaty deposits in Seewen and Bergsee for the more recent period. Lake Seewen was drained only about 200 yr after the AD 1356 Basle earthquake, and with a low sedimentation rate of 1.4 mm yr^{-1}, any recent soft sediment deformation would occur close to the present surface and would be destroyed by agricultural activities. In the case of Bergsee there is no opportunity for soft-sediment deformation to be preserved in the more peaty deposits in the uppermost core sections. Thus, the AD 1356 Basle earthquake, the possible AD 1021 event and the AD 250 *Augusta Raurica* event are not seen in the studied record. In addition, the speleological observations of Lemeille *et al.* (1999b) cannot be supported by the observations in Lake Seewen, which is only a few kilometres away from the investigated cave sites.

The preliminary identification of a number of AD 1356-type events for the period 0–11 000 BC indicates the long-term recurrence of damaging earthquakes in the Basle region and the assessment of regional seismic hazard. Based on the combined historical and palaeoseismological information available today, the conservative scenario would be four earthquakes in the last 13 000 yr, including the 1356 event and three pre-historical earthquakes; with a maximum scenario of eight earthquakes when the possible AD 1021 and the August Raurica earthquakes and five pre-historical events are included. An average recurrence time for an AD 1356-type event

would then range from 1500 to 3000 yr. The information available to date eliminates the more active seismicity scenarios depicted by curves A–B in Fig. 3 as well as the less active scenario of curve D, and constrains the possible activity rates for the Holocene and late Pleistocene period within a limited band (indicated by squares in Fig. 3).

Further investigations are needed to verify these observations, extending the lake investigations to a wider area and complementing them with fault trenching, rock fall and spelaeological investigations to obtain more precise identification and dating of events. However, this study provides some evidence for strong pre-historic earthquakes extending the instrumental and historical record in the Basle region as far back as the early Holocene and late Pleistocene.

ACKNOWLEDGMENTS

This project was funded by the ETH and Universität Zürich. We gratefully acknowledge the assistance in the field by Kurt Ruch and Willi Tanner of the Universität Bern (Geobotanik), Roger Perret (Universität Zürich) for the palynostratigraphic investigations, Souad Sellami for supplying data about the recent and historical seismicity of the Basle region, Walter Künzle and Urs Gerber (ETH Zürich) for assistance with core logging. We are also grateful for the support and provision of information by the landowners (Industrielle Werke Basel and Stadt Bad Säckingen). The preparation and pre-treatment of the samples for radiocarbon dating was carried out at the ^{14}C-laboratory of the Geographische Institut at the Universität Zürich (W.A. Keller, I. Woodhatch). The AMS with the tandem accelerator of the Institute of Particle Physics at the ETH-Hönggerberg was used for dating. Institut für Geophysik, ETH Zürich, contribution no. 1199.

REFERENCES

Alexandre, P., 1990. Les séismes en Europe occidentale de 394 à 1259, *Observatoire Royal de Belgique, Série Geophysique,* Bruxelles, p. 267.

Beck, C., Manalt, F., Chapron, E., Van Rensbergen, P. & De Baptist, M., 1996. Enhanced seismicity in the early post-glacial period: Evidence from the post-Würm sediments of lake Annecy, northwestern Alps, *J. Geodyn.,* **22,** 155–171.

Becker, A., Davenport, C.A., Haeberli, W., Burga, C., Perret, R., Flisch, A. & Keller, W.A., 2000. The Fulnau landslide and former Lake Seewen in the northern Swiss Jura Mountains, *Eclogae geol. Helv.,* **93,** 291–305.

Bonjer, K.-P., 1997. Seismicity pattern and style of seismic faulting at the eastern borderfault of the southern Rhine Graben, *Tectonophysics,* **275,** 41–69.

Boschi, E. *et al.*, 1996. New trends in active faulting studies for seismic hazard assessment, *Ann. Geofis.,* **XXXIX,** 1301–1307.

Camelbeeck, T. & Meghraoui, M., 1998. Geological and geophysicalevidence for large paleoearthquakes with surface faulting in the Roer Graben (northwest Europe), *Geophys. J. Int.,* **132,** 347–362.

Chapron, E., Beck, C., Pourchet, M. & Deconinck, J.-F., 1999. 1822 AD earthquake triggered homogenite in Lake Le Bourget (NW Alps), *TerraNova,* **11,** 86–92.

Davenport, C.A., 1993. Palaeoseismicity: hazard impact and research needs, Global Seismic Hazard Assessment Program (GSHAP) Regional Meeting, Nairobi, p. 9.

Davenport, C.A., 1994. Geotechnical consequences of ground motion: hazard perspectives, *Geol. Mijnbouw,* **73,** 339–356.

Davenport, C.A. & Ringrose, P.S., 1987. Deformation of Scottish Quaternary sediment sequences by strong earthquake motions, in *Deformation of Sediments and Sedimentary Rocks,* pp. 299–314, eds Jones, M.E. & Preston, R.M.F., Kluwer, Dordrecht.

Davenport, C.A., Ringrose, P.S., Becker, A., Hancock, P.L. & Fenton, C., 1989. Geological investigations of late and post-glacial earthquake activity in Scotland, in *Earthquakes at North–Atlantic Passive Margins: Neotectonics and Post-Glacial Rebound,* pp. 175–194, eds Gregersen, S. & Basham, P.W., Blackwell, London.

Doig, R., 1986. A method for determining the frequency of large-magnitude earthquakes using lake sediments, *Can. J. Earth Sci.,* **23,** 930–937.

Flisch, A. & Becker, A., 2002. Industrial X-ray computed tomography studies of lake sediment drill cores, *Geol. Soc. Lond. Spec. Publ.,* (submitted).

Furger, A.R., 1998. Augusta Raurica—durch ein Erdbeben zerstört?, *Augusta Raurica,* **98,** 6–9.

Gans, H.K., 1999. Kelten, Römer, Heizkanäle, *Archäologie Deutschland,* **1,** 60–61.

Haeberli, W., Schneider, A. & Zoller, H., 1976. Der 'Seewener See': Refraktionsseismische Untersuchung an einem spätglazialen bis frühholozänen Bergsturz-Stausee im Jura, *Regio Basiliensis,* **XVII,** 133–142.

Hajdas, I., Ivy-Ochs, S.D., Bonani, G., Lotter, A.F., Zolitschka, B. & Schlüchter, C., 1995. Radiocarbon age of the Laacher See Tephra: 11 230 ± 40 BP, *Radiocarbon,* **37,** 149–154.

Karnik, V., 1969. *Seismicity in the European area,* Part I, Reidel, Dordrecht.

Keefer, D.K., 1984. Landslides caused by earthquakes, *Bull. geol. Soc. Am.,* **95,** 406–421.

Lagerbäck, R., 1978. Neotectonic structures in northern Sweden, *Geol. Fören. Stockh. Förh.,* **100,** 263–269.

Lap, J.M.J., 1987. Earthquake-induced liquefaction potential in the area south of Eindhoven, the Netherlands, *Mem. Centre Eng. Geol. Netherlands,* **47,** 40.

Larsson, R., 1990. Behaviour of organic clay and gyttja, *Statens Geotekniska Institut Rapport,* **38,** p. 125.

Lemeille, F., Cushing, M.E., Cotton, F., Grellet, B., Ménillet, F., Audru, J.-C., Renardy, F. & Fléhoc, C., 1999a. Traces d'activité pléistocène des failles dans le Nord du fossé du Rhin supérieur (plaine d'Alsace, France), *C.R. Acad. Sci. Paris,* **328,** 839–846.

Lemeille, F., Cushing, M.E., Carbon, D., Grellet, B., Bitterli, T., Fléhoc, C. & Innocent C., 1999b. Co-seismic ruptures and deformations recorded by speleothems in the epicentral zone of the Basel earthquake, *Geodinamica Acta,* **12,** 179–191.

Lomnitz-Adler, J. & Lomnitz, C., 1979. A modified form of the Gutenberg–Richter magnitude–frequency relation, *Bull. seism. Soc. Am.,* **69,** 1209–1214.

Marco, S., Stein, M. & Agnon, A., 1996. Long-term earthquake clustering: a 50,000 year paleoseismic record in the Dead Sea Graben, *J. geophys. Res.,* **101,** 6179–6191.

Mayer-Rosa, D. & Cadiot, B., 1979. A review of the 1356 Basel earthquake, *Tectonophysics,* **53,** 325–333.

Meghraoui, M., Delouis, B., Ferry, M., Giardini, D., Huggenberger, P., Spottke, I. & Granet, M., 2001. Active normal faulting in the Rhine Graben and paleoseismic identification of the 1356 Basel earthquake, *Science* (in press).

Merkt, J. & Streif, H., 1970. Stechrohr-Bohrgeräte für limnische und marine Lockersedimente, *Geol. J.,* **88,** 137–148.

Metz, R., 1980. Geologische Landeskunde des Hotzenwaldes, Schauenburg, Lahr.

Meyer, B., Lacassin, R., Brulhet, J. & Mouroux, B., 1994. The Basel 1356 earthquake: which fault produced it?, *TerraNova,* **6,** 54–63.

Mörner, N.-A., 1985. Paleoseismicity and geodynamics in Sweden, *Tectonophysics,* **117,** 139–153.

Mörner, N.-A., Somi, E. & Zuchiewicz, W., 1989. Neotectonics and paleoseismicity within the Stockholm intracratonal region in Sweden, *Tectonophysics,* **163,** 289–303.

Obermeier, S.F., 1996. Use of liquefaction-induced features for paleoseismic analysis—an overview of how seismic liquefaction features can be distinguished from other features and how their regional distribution and properties of source sediment can be used to infer the location and strength of Holocene paleo-earthquakes, *Eng. Geol.,* **44,** 1–76.

Obermeier, S.F. & Pond, E.C., 1999. Issues in using liquefaction features for paleoseismic analysis, *Seismol. Res. Lett.,* **70,** 34–58.

Pantosti, D. & Yeats, R., 1993. The paleoseismicity of the late Holocene, in *Global Seismic Hazard Assessment Program (GSHAP) Technical Planning Volume,* eds Giardini, D. & Basham, P.W., *Ann. Geofis.,* **36,** 237–257.
Postpischl, D., Agostini, S., Forti, P. & Quinif, Y., 1991. Palaeoseismicity from karst sediments: the 'Grotta del Cervo' cave case study (Central Italy), *Tectonophysics,* **193,** 33–44.
Probst, E., 1991. Deutschland in der Steinzeit—Jäger, Fischer und Bauern zwischen Nordseeküste und Alpenraum, Bertelsmann, München.
Ringrose, P.S., 1989. Palaeoseismic (?) liquefaction events in lake sediments at Glen Roy, Scotland, *TerraNova,* **1,** 57–62.
Rodriguez-Pascua, M.A., Calvo, J.P., De Vicente, G. & Gomez-Gras, D., 2000. Soft-sediment deformation structures interpreted as seismites in lacustrine sediments of the Prebetic Zone, SE Spain, and their potential use as indicators of earthquake magnitudes during the late Miocene, *Sed. Geol.,* **135,** 117–135.
Rüttener, E., 1995. Earthquake hazard evaluation for Switzerland, *Geophysique,* **29,** 106.
Seilacher, A., 1969. Fault-graded beds interpreted as seismites, *Sedimentology,* **13,** 155–159.
Siegenthaler, C., Finger, W., Kelts, K. & Wang, S., 1987. Earthquake and seiche deposits in Lake Lucerne, Switzerland, *Eclogae geol. Helv.,* **80,** 241–260.
Sims, J.D., 1975. Determining earthquake recurrence intervals from deformational structures in young lacustrine sediments, *Tectonophysics,* **29,** 141–152.
Strahm, C., 1997. Chronologie der Pfahlbauten, in *Pfahlbauten rund um die Alpen,* pp. 124–126, ed. Schlichtherle, H., WBG, Darmstadt.
Sturm, M., Siegenthaler, C. & Pickrill, R.A., 1995. Turbidites and 'homogenites'—a conceptual model of flood and slide deposits, 16th European Regional IAS Meeting/Aix-les-Bains/France/24–25 April, **22,** 170–171.
Van den Bogaard, P., 1995. $^{40}Ar/^{39}Ar$ ages of sanidine phenocrysts from Laacher See Tephra (12,900 yr BP): Chronostratigraphic and petrological significance, *Earth planet. Sci. Lett.,* **133,** 163–174.
Van den Bogaard, P. & Schmincke, H.-U., 1985. Laacher See Tephra: a widespread isochronous late Quaternary tephra layer in central and northern Europe, *Bull. geol. Soc. Am.,* **96,** 1554–1571.
Vittori, E., Labini, S.S. & Serva, L., 1991. Palaeoseismology: review of the state of the art, *Tectonophysics,* **193,** 9–32.
Wells, D.L. & Coppersmith, K.J., 1994. New empirical relationships among magnitude, rupture length, rupture width, rupture area, and surface displacement, *Bull. seism. Soc. Am.,* **84,** 974–1002.
Young, R. & Coppersmith, K., 1985. Implications of fault slip rates and earthquake recurrence models to probabilistic seismic hazard estimates, *Bull. seism. Soc. Am.,* **75,** 939–964.

APPENDIX A

Event horizons in Lake Seewen

Event horizon S1 is seen best in SL2.2 (Fig. 6), as well as in SL2.3, at a depth around 2.10 m. In both boreholes S1 starts with a horizontal thin sand layer (0.5 cm) above a maximal 1 cm thick layer rich in plant remains. Above, a bed of sand dips at 11° at its base and at 24° at the top, creating a wedge of sand embedded in silty sands. Further up, the horizon is completed by silty sands, sandy silts and silts and finally silty clays with a nebulous and nebulous-spotty texture. The sequence from 2.03 to 2.17 m in SL2.2 is very rich in plant remains, e.g. pieces of wood, leaf fragments and indeterminable plant chaff. Radiocarbon dates point to fast sedimentation, i.e. at 1.84 m 1435 ± 60 BP, at 2.14 m 1465 ± 60 BP. Based on radiocarbon dates, S1 correlates with the onset of lake sedimentation at site SL4 (Fig. 4). The earliest deposits encountered in SL4 could be periglacial debris, talus from the valley flanks or a coarse-grained fluviatile deposit close to the former mouth of the river Seebach. S1 marks the beginning of a high lake level stand, caused by the rise of the dam at the western end of the lake, possibly caused by the *Welschhans* rock fall (Fig. 3) (Becker *et al.* 2000).

Event horizon S2 was detected only in SR1 (Fig. 6) in a very homogeneous lacustrine silty clay sequence. The base of S2 is not visible owing to a gap in the core recovery. The horizon consists of silty sands rich in plant material and shell fragments (mostly gastropods) from 6.98 to 6.80 m (Fig. 6). In the lower part there are vague irregularly bedded thin silty sand layers. Above S2 three thin dark grey to black layers suggest abundant organic material. Shell fragments, isolated lumps of organic material and the irregular (cross-bedded?) silty sand layers indicate a higher-energy lacustrine sedimentary environment compared with the common silty clay deposits. This event seems to be caused by very local sedimentary conditions, occurring only in the western lake basin. Radiocarbon dating revealed an age of 5630 ± 65 BP.

Event horizon S3 is shown in Fig. 7 which depicts the situation in SR1. The horizon starts at 8.92 m as an uneven contact between sandy silts and underlying clays to silty clays. The sandy silt layer dips at 10° and shows a sharp contact with the overlying 1 cm thick sand layer. The wedge-shaped silty sand layer at the top of the event horizon has a horizontal upper boundary at a depth of 8.82 m. The whole sequence is rich in plant remains and also contains shell fragments. Correlation between SR1 and SL2.1 is based on radiocarbon dates, i.e. 6410 ± 60 BP in SR1, and in SL2.1 at 8.44 m 6360 ± 75 BP and at 8.20 m 6415 ± 60 BP. In SL2.1 there are two horizons, the lower one consisting of an 11 cm thick gravel deposit that includes rounded pebbles and cobbles of *Hauptrogenstein* limestone, calcsinter and Jurassic fossils. The gravel is overlain by 19 cm of homogeneous silty clay to silt, followed by the second horizon of 23 cm of silt with small black particles (charcoal, wood) including white grains of limestone and a black layer with plant remains. Because the radiocarbon ages do not allow us to separate the two layers from each other, the lower gravel layer is correlated with the silty-sandy layer in SR1 around 8.90 m. This suggests a westward grading of sediments from Seebach mouth gravel to silty sand in the distal deepest part of the lake. Therefore, it is likely that this horizon represents an extraordinary flood event, encouraged by human activity. Dendrochronologically calibrated radiocarbon ages of about 5300–5400 BC support this interpretation, i.e. a flood at the start of early Neolithic deforestation and agriculture in northern Switzerland (Probst 1991).

In SR1, event horizon S4 consists of a grading-upward layer of sands at the base (9.91 m) and silty sands at the top (9.84 m), with thin layers of dark-grey organic rich material (Fig. 7). In the sediment underlying the event horizon a dark lump of organic material is embedded resembling a rhizome of a plant. S4 has been correlated with the onset of sedimentation in borehole SL2.1 at a depth of 9.45 m, but could not be proven by dating. It seems that S4 is an exceptional flood event at the beginning of a general lake level rise.

Event horizon S5 occurs only in SR1 at a depth between 16.36–16.61 m. At the base, a horizontal 4 cm thick clay to silty clay containing small fissures overlies a silt sequence containing thin organic layers (Fig. 7). This is followed by a 0.5–1 cm thick silt layer which thickens rapidly up to 5 cm at the left-hand side of the drill core. At the steep edge of the thicker part of the silt layer a small fissure can be seen in the X-ray radiogram. Above the silt layer a few tiny fissures are also found in the clay and silty clay containing discontinuous thin dark layers and silt layers. Higher up, a continuous thin (5 mm), slightly inclined, undulating silt layer is overlain by two 22° dipping disrupted silt and sandy silt layers (Fig. 8). The two layers on the right-hand side show dome-like

structures and the upper layer on the left-hand side contains two thin clay to silty clay intercalations. Many small fissures are seen in X-ray radiograms and tomograms (Fig. 9), some of which appear to be linked to the upper domed layer and are also found up to the top of S5. The whole event horizon contains virtually no organic macroremains, so that radiocarbon dating is impossible. However, the pollen grains are well preserved and their concentration (pollen grains cm^{-3} of sediment) is up to six times higher at a depth of 16.49 m and three to four times higher between 16.44 and 15.90 m compared with the average in the drill sections between 18 and 7 m. These increased pollen concentrations are considered to partly reflect the dramatic changes in the vegetation at the transition from Pleistocene to Holocene (Younger Dryas/Allerød transition), and may also reflect reduced sedimentation rates at that time. The high degree of preservation of the pollen grains indicates that they have not suffered aerobic conditions and that the lake must have experienced continuous but reduced sedimentation. Therefore, S5 is unlikely to contain flood events. The most significant feature of the event horizon is the deformation structure seen as disrupted, folded and tilted silt layers within a continuous matrix of normal lacustrine background sediment (Fig. 8). The shape and relationships of the layers are similar to parts of liquefaction-induced structures reported from lake sediments elsewhere (Davenport & Ringrose 1987). The small fissures, which appear to be connected to the liquified layers, could be interpreted as small water escape structures. These observations combined with the evidence of an environment of normal to low sedimentation rates point to *in situ* deformation, probably caused by strong ground motion.

Event horizon S6 is developed between 17.10 and 17.40 m in SR1. This succession starts with silty clay and thin dark layers followed by silt, sandy silt, silty sand and then again a silt layer (Fig. 6). The remainder of the succession is a thin silty clay followed by silt and then silty clay to clay again. In the lower and upper silt layers, subangular pebbles of limestone referred to as dropstones, are common. These are also found in the silty clay and clay below and above the event horizon, along with occasional large plant remains (wood, charcoal). Plant remains are frequent in the section below 17.30 m, but rare above. The coarser layer in the middle part shows a slight dip and uneven contacts, above which fissures can be seen in X-ray tomograms and radiograms. In the clays and silty clays containing dropstones above 17.24 m, fissures seem to be partly nucleated at dropstones, may be caused by differential compaction and stress concentration at the edges of the dropstones. However, immediately above the coarse-grained layer no dropstones can be seen but there are some fissures. Furthermore, below this layer, dropstones are also common but fissures are missing completely. This observation seems to indicate that fissures are not necessarily genetically linked to the occurrence of dropstones. The pollen concentration is low (Becker *et al.* 2000), some samples are close to the lower limit of the average in SR1, indicating generally higher sedimentation rates. Radiocarbon ages at depths of 17.19 m ($10\,205 \pm 95$ BP), 17.31 m ($10\,360 \pm 90$ BP), 17.34 m ($10\,525 \pm 105$ BP) and, finally, at 17.50 m ($10\,705 \pm 95$ BP) support this interpretation. This suggests increased sediment supply, possibly as a result of the breakup and melting of an ice cover, releasing dropstones, and a rapid input of fine-grained clastic material afterwards. Because the small fractures that can be seen in X-ray radio- and tomograms are unlikely to be formed in this depositional environment or by differential compaction as discussed above, another explanation is required. One possibility is that the fractures were formed later by earthquake shaking, possibly as late as the shaking event shown in S5.

Event horizon S7 starts with silty sands (17.58 m) above a silty clay and grades upwards into silts and finally into silty clays at its top (17.49 m). Below and above the event horizon dropstones, rare wood fragments and dark layers can be seen. Radiocarbon dates at 17.50 m supply an age of $10\,705 \pm 95$ BP and at 17.61 m an age of $10\,790 \pm 95$ BP, indicating rapid sedimentation of the coarser-grained layers, possibly related to a flood event.

Event horizon S8 is developed in SR1 between 18.20 and 18.40 m (Figs 5 and 6). The succession starts with thin silt layers and three intercalated dark-grey clay layers, followed by two sequences of more coarse-grained sediments, starting above a thin clay layer with silty sand, silty clay to silt, again repeated as silty sand, silt and silty clay (Fig. 7). The top silty clay contains a thin dark-grey discontinuous and upturned clay layer. Further up another silt layer is included in the silty clay. Within the silty sand and silt layers, clay clasts are frequent. Additionally, below a depth of 18.29 m, the sequence is rich in organic material down to 18.35 m, where plant fibres and wood fragments are concentrated in very thin layers. In the upper and lower parts of the succession, dropstones are common, which are not seen in the coarser sediments of the event horizon. Small fissures occur within the vicinity of the thin, broken and upturned dark layer. The pollen concentration of three samples is lowest in the deepest sample at 18.40 m and highest at the top sample at 18.25 m. Radiocarbon ages in the lower part of the event horizon are very close and indicate an age inversion which, statistically, is not significant because the data are still within the limits of the standard deviation, i.e. a wood fragment at 18.40 m, giving $11\,140 \pm 100$ BP and plant fibres at 18.32 m, giving $11\,240 \pm 100$ BP (Becker *et al.* 2000). This indicates a very fast and dynamic sedimentation regime in which older deposits (clay clasts) are reworked and mixed with some organic material. Above 18.29 m the sedimentary conditions changed to permit the deposition of clay. This grading sequence with coarse-grained material at the base and fine-grained material at the top indicates an upward decrease of permeability, with the thin dark-grey clay layer acting as a permeability barrier in its originally intact condition. The disruption of this impermeable layer can be interpreted as a water escape structure, caused by the upward movement of sediment and water either as a result of increasing sediment load or seismic shaking. Confirmation of upward injection is provided by the presence of a subvertical fissure with a silty infill from 18.275 to 18.265 m, below and within the breach of the upturned clay layer (Fig. 7).

Event horizon S9 is developed in SR1 between 18.75 and 18.60 m. The clays and silty clays above and below the event horizon contain dropstones, organic macroremains (wood) and dark-grey layers. The event horizon starts with a sandy silt without plant remains, followed by a repeated sequence of silty clay and silty sand, and terminating with a sandy silt, all rich in organic material (Fig. 7). The layers show undulating boundaries, most obvious for the middle silty sand layer. Most intriguing is a nest of silty sand at the base of the lower sandy silt layer, which can be linked with a small dyke (Figs 6 and 9) and traced, at least, down to a small gap in the core (which is caused by drilling). Below that gap, again two small traces of a silty dyke can be seen. Between the end of this core and the beginning of next (deeper) core section, there is a 14 cm gap with no recovery followed by 12 cm disturbed recovery. This gap could have contained a sand layer, but there is no supporting evidence. However, the consistent appearance and continuity of the dyke can be demonstrated from X-ray tomograms, suggesting that the silty infill is more likely to be derived from upward injection. The pollen concentration at 18.74 m in silty clay is about twice as high as at 18.67 m within the silty sand, indicating a higher

sedimentation rate for the sandy layer, presenting the possibility of a flood event in S9. Although the small sand dyke and its upward termination may be the result of a simple dewatering by rapid loading of the unconsolidated sediments beneath, it is equally likely that the injection has a 'seismogenic' origin. In both cases the 'nest'-layer may represent a 'sill'-like deposit at the limit of injection pressure. Only in the case of earthquake shaking is there an alternative, i.e. the nest represents a surface extrusion feature. The nature of the sedimentary contact above the nest favours this interpretation.

Event horizons in Lake Bergsee

The event horizons described in this section are from the sediments of the Holocene and latest Pleistocene. Based on macroscopic lithological descriptions and X-ray tomograms, five event horizons can be distinguished, four of them are related to zones of increased fracturing, and the other is a discontinuous sandy silt layer. They are numbered with B1–B5 from top to base (Fig. 11).

Event horizon B1 was detected at a depth of about 3 m (Fig. 11). In each of BL2.2 and BL3.1, which are about 80 m apart, an open crack can be seen, partly filled with sand, the latter dipping at 45°. In BL1.1 and BL1.2, slightly deeper zones with small fractures or irregularly broken core sections occur, which are partly caused by drilling. Nothing could be seen in BL2.1 other then small sand concentrations. The sediments in the vicinity of the fractures have radiocarbon ages of between 2995 ± 50 and 3360 ± 50 BP.

The event horizon B2 is seen in three of the five boreholes, generally between 5 and 6 m (Fig. 11). In BL1.1 it is questionable whether the essentially horizontal fractures are natural. The preferred explanations are disturbance by drilling or core expansion. BL1.2 presents homogenous material, so that it is virtually impossible to detect any deformation features. Only with the aid of X-ray tomograms can small cavities, sometimes cracks, be seen. Some of the features can be accounted for as small root tubes or bubble tracks owing to degassing. In BL2.1 probably only the lower fractures related to B2 are natural. One higher crack contains white coarse-grained angular feldspar fragments at a depth of 5.65 m and small sand pockets occur in two other cracks. However, these sandpockets are not injection-like structures but simple sedimentary accumulations. Therefore, it is believed that these fractures are caused by core expansion following inhomogeneities in the gyttja, giving a false impression of 'open cracks filled by sand grains and pockets'. The radiocarbon age of the sediments in the vicinity of the cracks is about 5200–5600 BP.

Event horizon B3 is developed only in the two neighbouring boreholes BL1.1 and BL1.2. In BL1.1, a 35 ° dipping crack is seen, which contains a pocket of quartz and feldspar sand at 7.40 m, and between 7.68 and 7.81 m, six cracks with dips between 40° and 50°, increasing downwards. A narrow zone of disturbance is seen in BL1.2 as well. Between 7.70 and 8.20 m, three sections with small cracks and fissures are developed. Additionally, there is an irregularly fractured zone between 8.80 and 8.90 m. No such deformation features are seen in the remaining three boreholes. The radiocarbon age of the sediments is about 7000 BP.

Event horizon B4 occurs at a depth between 10 and 11 m in general where clear evidence is found for the natural origin of some fractures. In BL1.1 at a depth between 10.18 and 10.32 m, two fractures with white and pale greenish blue mineral coatings in flecks are seen. In BL3.1 an irregular open fissure includes blue mineral deposits (vivianite) at a depth of 11.52 m. In BL2.2 a 35° dipping fracture occurs between 10.23 and 10.34 m, above which subvertical cracks in two thin gyttja layers can be seen and below which there are unevenly distributed small horizontal cracks. However, the lower horizontal cracks could be related to core expansion during recovery. Subhorizontal cracks are also found in BL2.1 at about the same depth interval as in BL2.2 and BL1.1, however, without clear evidence for a natural origin. Cracks are not seen in BL1.2. Altogether three of the five boreholes (BL1.1, BL2.2, BL3.1) contain the most likely natural fractures, all within the same depth range.

Event horizon B5 is the only prominent sedimentary horizon among the Bergsee event horizons, occurring at a depth of about 13 m in all three boreholes which reach this depth (Fig. 11). This horizon varies from 10 cm (BL1.1) to 50 cm (BL1.2) seen as several thin layers of whitish sandy silt. These layers show dips of between 5° and 15° and are generally continuous with vertical connections in places. Paleomagnetic investigations of the cores reveal the presence of ferromagnetic minerals in some samples of B5. In thin sections, the lighter coloured layers contain tephra in the form of glassy pumice fragments with inclusions of feldspar and amphibole (Schmincke, personal communication 1999). The presence of tephra in these layers suggests a correlation with the well-known Laacher See event, a phreatomagmatic-plinian volcanic eruption in the Eifel Mountains of western Germany, about 320 km north of Lake Bergsee (Van den Bogaard & Schmincke 1985; Van den Bogaard 1995). The radiocarbon ages of between 11 300 and 11 700 BP support this conclusion (Hajdas *et al.* 1995). In general, the Laacher See Tephra (LST) is only a few millimetres thick in Switzerland and the southern Black Forest. However, the whole sandy silt layer sequence must account for more than the LST, suggesting that some additional clastic input into the lake occurred at this time. Whether the structural connections between layers are purely of sedimentary origin or a result of soft-sediment deformation is not yet clear. However, BL3.1 shows an irregular fracture with a dip of 30° and local blue mineral coating (vivianite?) about 1 m below event horizon B5.